Master thesis performed at:

GHENT UNIVERSITY
FACULTY OF PHARMACEUTICAL SCIENCES
Department of Pharmaceutics
Laboratory for General Biochemistry and Physical Pharmacy

UNIVERSITY OF MINHO
SCHOOL OF SCIENCES
CFUM - Centre of Physics

Academic year 2013-2014

BOVINE SERUM ALBUMIN (BSA) ENCAPSULATED IN DODAB:MO (1:2) LIPOSOMES FOR TARGETED DRUG DELIVERY: DEVELOPMENT AND CHARACTERISATION

Ann VAN DIJCK

First Master of Drug Development

Promoter:

Prof. dr. K. Braeckmans

Co-Promoter:

Prof. dr. M.E.C.D.R. Oliveira

Commissioners:

Prof. J.P. Remon

Dr. K. Raemdonck

GHENT UNIVERSITY

FACULTY OF PHARMACEUTICAL SCIENCES

Department of Pharmaceutics

Laboratory for General Biochemistry and Physical Pharmacy

Master thesis performed at:

UNIVERSITY OF MINHO

SCHOOL OF SCIENCES

CFUM - Centre of Physics

Academic year 2013-2014

BOVINE SERUM ALBUMIN (BSA) ENCAPSULATED IN DODAB:MO (1:2) LIPOSOMES FOR TARGETED DRUG DELIVERY: DEVELOPMENT AND CHARACTERISATION

Ann VAN DIJCK

First Master of Drug Development

Promoter:

Prof. dr. K. Braeckmans

Co-Promoter:

Prof. dr. M.E.C.D.R. Oliveira

Commissioners:

Prof. J.P. Remon

Dr. K. Raemdonck

ABSTRACT

The main purpose of this project is the development and characterisation of a nanoparticle system with a new composition that allows a site-specific drug delivery in the body in an efficient way. The carrier system consists of lipid nanoparticles encapsulated with bovine serum albumin (BSA). BSA is a natural carrier protein in mammals. The encapsulation of liposomes with BSA improves the loading and releasing efficiency of several drugs.

Various formulations of liposomes have been created and tested before. This project focuses on the development of liposomes consisting of Dioctadecyldimethylammonium Bromide (DODAB) and 1-oleoyl-rac-glycerol (Monoolein (MO)). Different DODAB:MO ratios have been studied and used before, in this work a DODAB:MO ratio of (1:2) will be used. The aim of this project is to discover which BSA/DODAB:MO (1:2) ratio shows the best results in stability, encapsulation efficiency and release.

The stability of different BSA/lipid ratios is evaluated by measuring the size and zeta potential of the liposomes. The encapsulation of liposomes with BSA has not got a turnover of 100%. The encapsulation efficiency is determined through ultraviolet/visible spectrophotometry and fluorescence. BSA can be encapsulated inside the liposomes and/or attached to the outside surface of the liposomes. To determine where the BSA molecules are located the BSA partition coefficient is calculated. To study the molecular structure of the DODAB:MO liposome and the changes which occur by BSA encapsulation, circular dichroism is measured.

The stability and encapsulation efficiency are different for each BSA/lipid mole ratio. The liposomes with less protein (0.752) proved to be the most stable protein/lipid ratio with the highest encapsulation efficiency. The BSA/lipid mole ratios of 0.968 and 0.987 also show satisfying results.

In the near future, the controlled release assay will be carried out. This quantification of BSA in media with different pH will be used in *in vitro* controlled release assays on cell cultures which are planned to be carried out in continuation of the current work.

SAMENVATTING

Deze masterthesis handelt primair over de ontwikkeling en de karakterisering van een nanodeeltje met een nieuwe samenstelling. Het doel is de ontwikkeling van een nanocarrier dat bepaalde geneesmiddelen op een efficiënte manier op een specifieke plaats in het lichaam kan afgeven. Het carrier systeem bestaat uit liposomen in dewelke BSA wordt geïncorporeerd. BSA is gekend als een dragerproteïne en zal de belading en afgifte van de geneesmiddelen in het lichaam bevorderen.

Er zijn reeds verscheidene liposomen met verschillende samenstellingen ontwikkeld en getest voor diverse doeleinden. Tijdens dit project zal een nanopartikel bestaande uit Dioctadecyldimethylammonium Bromide (DODAB) and Monoolein (MO) ontwikkeld worden. Er zijn al meerdere ratio's onderzocht geweest, echter nu ligt de focus op een DODAB:MO ratio van (1:2). Er wordt bestudeerd welke BSA/DODAB:MO (1:2) verhouding de beste resultaten oplevert betreffende stabiliteit, efficiëntie van inkapseling en vrijgave in het lichaam.

De stabiliteit wordt opgevolgd door de partikel grootte en zeta potentiaal van de liposomen te meten en op te volgen. Helaas is het rendement van de BSA incorporatie in de liposomen niet gelijk aan 100%. Daarom wordt de efficiëntie berekend op basis van UV-VIS spectrofotometrie en fluorescentie. BSA kan naast incorporatie ook geadsorbeerd worden aan het oppervlak van de positief geladen liposomen. Om de exacte locatie van de proteïne te bepalen wordt de BSA partitiecoëfficiënt bepaald. Door de inkapseling en/of de adsorptie verandert de moleculaire structuur van de nanopartikels. Deze verandering wordt bestudeerd via circulair dichroïsme.

De liposomen met een BSA/lipid molaire ratio van 0.752 zijn het stabielste en vertonen de hoogste efficiëntie betreffende de BSA incorporatie. Ook de monsters met een BSA/lipid molaire ratio van 0.968 en 0.987 geven bevredigende resultaten.

In de toekomst zal de hoeveelheid aan BSA dewelke vrijkomt in bepaalde lichaamsvloeistoffen bepaald worden. De preparaten kunnen nadien *in vitro* getest worden op celculturen.

ACKNOWLEDGEMENTS

First and foremost, I would like to give my deepest appreciation to Apr. Dr. Marlene Lucío for sharing her knowledge with me. She offered me an incredible support and guidance. I thank her for the huge effort in these last days. Without her this project and paper would not have been what it is now.

I want to express my sincere gratitude to Professor Elisabete Oliveira for giving me the opportunity to join her research group and receiving me so well.

I want to thank my brother for the time and effort he put in helping me. I appreciate his support and efforts to cheer me up when everything seemed too hard and difficult.

I would like to express my love and gratitude to my parents, for making it possible for me to go abroad. Their support meant a lot to me, even if it was from a distance. I also want to thank them for their everlasting support during my whole academic education and not only for the last four months.

I could always count on the support of my colleagues in the laboratory when I needed appliances, professional advice or just a talk. Thank you for that.

Last, but not least, I would like to thank the friends that I made in these last few months. They reminded me to relax once and a while after a long working day. They were my sunshine when skies were grey. I will miss you Erasmus Uminho.

TABLE OF CONTENTS

LIST OF ABBREVIATIONS

BSA	Bovine serum albumin
CdTe	Cadmium telluride
DLS	Dynamic light scattering
DODAB	Dioctadecyldimethylammonium bromide
DOPE	Dioleoylphosphatidylethanolamine
ELS	Electrophoretic light scattering
FITC-BSA	Fluorescein isothiocyanate – conjugated bovine serum albumin
Folate-PEG-g-TMC	Folate-poly(ethylene glycol)-grafted-trimethylchitosan
GL-BSA-HCPT-NP	glycyrrhizic acid
HAS	Human serum albumin
HCPT	10-hydroxycamptothecin
HLB	Hydrophobic lipophilic balance
K_p	Partition coefficient
λexc	Excitation wavelength
LUV	Large unilamellar vesicles
MLV	Multilamellar vesicles
MO	Monoolein or 1-oleoyl-rac-glycerol
MPA	Mercaptopropionic acid
MWCO	Molecular weight cut off
NIR	Near Infrared
NMWL	Nominal molecular weight limit
NP	Nanoparticles
PCN	Polyelectrolyte complex nanoparticle
PDI	Polydispersity index
pDNA	Plasmid deoxyribonucleic acid
PEG	Polyethylene glycol
PLGA	Poly(lactic acid-co-glycolic acid)
PPD	Poly(vinyl pyrrolidone)-graft-poly(2-dimethylaminoethyl methacrylate)
PSD	Particle size distribution
QD	Quantum dot

St.Dev.	Standard deviation
SUV	Small unilamellar vesicles
TCC	Temperature controlled cell holder
Tm	Gel-to-liquid crystalline phase transition temperature
UV	Ultraviolet
VIS	Visible

LIST OF EQUATIONS

LIST OF FIGURES AND TABLES

1. INTRODUCTION

1.1. NANOPARTICLES AND LIPOSOMES

Nanoparticles have been a topic of interest since many decades. Nanogels, nanospheres, liposomes and many more nanoparticles have been developed and researched. They are commonly used in physics, but also in life sciences. Bioimaging, diagnostics and therapeutic purposes such as vaccines, gene silencing and drug delivery systems are just a few fields in which nanoparticles can be used (1).

The beginning of the research on liposomes started in 1961, when A. D. Bangham, a British haematologist at the Institute of Animal Physiology in Cambridge, now called the Babraham Institute, discovered liposomes by testing the institute's new electron microscope. By adding a negative stain to dry phospholipids, he and R.W. Horne discovered that phospholipids organise themselves into double layers in an aqueous environment (48). These double layer vesicles are now called liposomes and are made up of phospholipids.

Phospholipids are amphiphiles because of their dual chemical nature with distinct polarity. They are made up of a hydrophobic and a hydrophilic molecular part. If the concentration of phospholipids is greater than or equal to the critical micellar concentration (CMC) and the temperature is above the Krafft temperature, amphiphilic molecules can form micelles (2). Micelles are aggregates of amphiphilic molecules, but consist only of one monolayer. In an aqueous compartment, the hydrocarbon chains of all the phospholipids are repelled because of the hydrophobic effect and will turn themselves inwards. The hydrophilic parts will be facing the outside in such way that the hydrophobic parts are separated from the aqueous environment (71, 72).

The molecular shape of the vesicle which is formed depends on several factors, such as the temperature, water content and chemical structure of the phospholipid. Different names are given to the vesicles, dependent on the critical packing parameter or shape factor (γ).

$$\gamma = \frac{v}{á_0 \cdot l_c} \quad (1.1)$$

In which: v = molecular volume

l_c = effective maximum chain extension

α_0 = optimum headgroup area

Most preferred geometries of amphiphiles are spherical, cylindrical, lamellar and inverted. They are written down in increasing hydrophobic character (49).

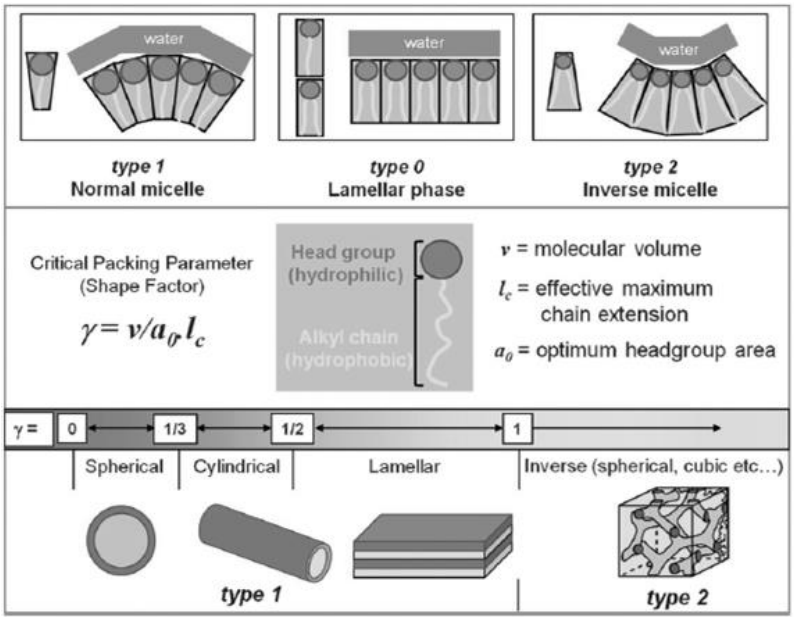

Figure 1.1 Shape types of liposomes corresponding with their critical packing parameter (*γ*) (2)

The critical packing parameter can vary from 0 until values higher than 1. When *γ* has a value between 0 and 1/3 most likely spherical micelles will be formed because the entropy of this geometry is favoured. When *γ* is between 1/3 and 1/2, cylindrical micelles are favoured, again because of their entropy. In this range of the critical packing parameter, also vesicles and bilayers can exist, spherical micelles on the other hand cannot. When the shape factor increases, cylindrical micelles are also not able to be formed anymore. Only bilayers and vesicles are entropically able to exist. Vesicles are favoured if the value ranges between 1/2 and 1. When the packing parameter is 1, the vesicles enlarge and it will not be able to distinguish them from planar bilayers. Greater values give rise to inverted structures, such as inverted micelles that can polymerise and give rise to hexagonal phases (also called type II) and cubic phases (49). 'Type II' refers to the fact that there is a curvature towards the water region, a phenomenon called 'inverse' (2, 3).

Lipid vesicles are very interesting not only for their drug delivering properties, but also because they can mimic the actual biophysical and chemical environment found inside the human body. Indeed, the inside and outside of a cell is constituted of an aqueous environment. The phospholipids of cell membranes form a bilayer consisting of two monolayers in which the non-polar, hydrocarbon chains are shielded from the water and face each other, while the polar, hydrophilic groups of the phospholipid are attracted to the water in both the inside and outside of the cell. Cellular membranes are essentially lamellar bilayers that do not show any curvature towards water nor towards the hydrocarbon chain region, thus they have the property of being flat (2, 72).

1.2. LIPOSOMES

1.2.1. Characteristics

Since decades scientists discovered that liposomes could encapsulate drugs, nutrients and other bioactive compounds. The type of content on the inside of the liposome depends on which kind of vesicle structure is used. Liposomes are made of amphiphilic molecules; this makes it possible for them to be a carrier of amphiphilic, lipo- and hydrophilic molecules. The only difference between them will be the localization in the particle (4). Molecules can either adsorb on the surface of the liposomes, they can stay in the lipophilic region formed by the hydrocarbon chains, or they can be encapsulated in the hydrophilic compartment.

When the encapsulated compound is a therapeutic agent, liposomes offer the advantage of protecting both the drug and the body against each other influences. Furthermore, liposomes are able to stabilise the encapsulated molecules against chemical and environmental influences. They are able to reduce the toxicity of the encapsulated molecule as well as to enhance the clinical effect of it. Moreover, liposomes are biocompatible, biodegradable, show a low toxicity and are non-antigenic. The fact that they have a long plasma half-life makes the nanoparticles very useful for controlled release systems. Also site specific drug delivery is possible. When liposomes are intravenously injected, most of them cumulate in the bone marrow, lymph nodes, spleen, lungs, and liver. Liposomes can accumulate in pathological areas where there is little blood flow, such as

some solid tumours and sites of inflammation and infection. The liposomal carrier is able to transport itself across biological membranes because of its small particle size. The drug can be delivered to the site of action through certain membrane surface modifications, such as fusion, adsorption, endocytosis or lipid exchange (5, 6).

To use liposomes *in vivo* it is important to verify some characteristics of the preparations. Size and size distribution are very important features. A homogenous distribution of small particles is desired. Nanoparticles are cleared from the bloodstream by macrophages of the reticuloendothelial system. It is at the liver and the spleen that most of the clearance occurs, because the macrophages are in direct contact with the blood stream in those two organs. The time upon which the liposomes are eliminated depends on their size, surface characteristics and lipid composition. In general it takes less than one hour to eliminate more than fifty percent of intravenously injected liposomes (7). The use of nanoparticles in *in vivo* applications also depends on their drug loading, biodistribution, targeting (partition coefficient), therapeutic efficacy and their half-life (50). Surface stabilisation by means of non-ionic surfactants or polymeric macromolecules has proven to be successful in extending the half-life (8).

1.2.2. DODAB:MO (1:2) liposomes

The liposomes that are researched in this project are made up of dioctadecyldimethylammonium bromide (DODAB) and monoolein (MO) in a particular ratio of one to two. The combination of both lipids proves to be a promising nanoparticle to carry drugs. DODAB is a widely used monovalent cationic surfactant in liposomes. It consists of a double saturated acyl chain (C18:0) which is attached to a quaternary ammonium group. This latter hydrophilic part gives the positive charge to the lipid. It is a bilayer forming surfactant with a high gel-to-liquid crystalline phase transition temperature (T_m) of 45°C (9, 10).

The fluidity of lipid bilayers and the individual mobility of a single lipid in that bilayer is characterised by the lipid phase behaviour. Every lipid has its own gel-to-liquid crystalline phase transition temperature (T_m) value. Below this temperature the lipid is in a solid-crystalline or 'gel' phase, above the T_m it is in a liquid-crystalline or fluid phase. In the liquid-

crystalline phase, the lipids are able to diffuse freely within its plane. This property makes the lipids receptive for drugs to be encapsulated (62).

The high transition temperature of DODAB makes DODAB liposomes highly ordered at the human body temperature (37°C). This feature has the advantage of producing highly stable liposomes that can keep drugs circulating in the body without their instant release. However, the increased rigidity of DODAB liposomes may also have the disadvantage encapsulating less drug. This latter limitation can be attenuated by adding a helper lipid with a lower T_m to the formulation. Examples of such helper lipids are monoolein (MO), cholesterol and dioleoylphosphatidylethanolamine (DOPE) (11, 50).

MO is an emulsifying agent, used as a food additive. In 1984, monoolein was presented for the first time as a biocompatible encapsulating material with controlled-releasing properties. It is a neutral amphiphilic molecule with a C18 hydrocarbon chain with a *cis* double bond at position 9,10 (oleic acid). The *cis* orientation of the double bound causes the alkyl chain to have a bigger sterical effect, which leads to the formation of inverted structures if the shape factor (γ) is greater than one. A glycerol molecule is attached to the hydrocarbon chain with an ester bond. It has two free hydroxyls left which creates the hydrophilic part of the molecule. The hydrophilic lipophilic balance (HLB) of MO is 3.8 (2, 12).

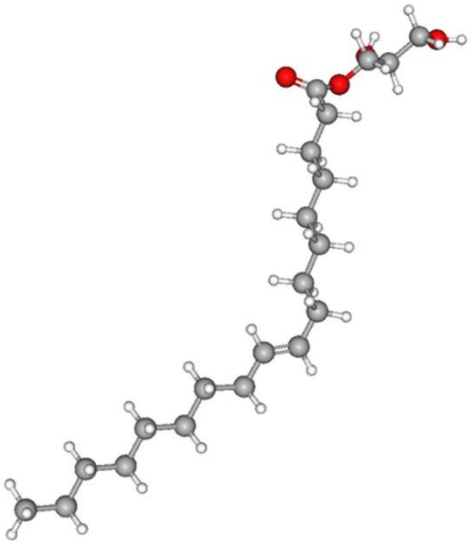

Figure 1.2 Monooleine. Drawn with MarvinSketch

MO exhibits two inverted bicontinuous cubic phases and as a result MO forms non-lamellar vesicles with negative curvature. This characteristic decreases the structural rigidity of DODAB vesicles. It causes an increase in the lateral mobility of the lipid chain which in his turn causes an improvement in the fusion of the liposomes with the cell membrane (10). The change of the vesicle into an inverted non-lamellar structure also facilitates the release of the vesicular content (60). Tuning MO content in DODAB:MO formulations is also very advantageous in terms of formulation development for drug delivery purposes. Therefore,

the ratio DODAB:MO (1:2) used in this work promotes the formation of lamellar phases of DODAB containing MO in inverted non-lamellar phases. This way the vesicle will have both a structural rigidity (required for retaining the compounds encapsulated) caused by DODAB lamellar phase, and a fluid content (interesting for encapsulation purposes) as a consequence of the MO inverted non-lamellar phases.

In lipoplexes, MO is also useful to reduce the net positive charge. The positive charge is necessary for the complexation of nucleic acids. This charge reducing effect is correlated with a decrease of transfection-associated cytotoxicity (50). The net positive charge of DODAB:MO (1:2) formulation is essential for two motives. First, it will favour the electrostatic interactions with BSA because of its negatively charged surface. Second, it will promote the binding of the vesicles to the cell surfaces membrane which are slightly negative. Other interesting characteristics of MO are its low cost, non-toxicity and biocompatibility. MO is also biodegradable because of the esterase activity in many body tissues (2, 12).

1.3. BOVINE SERUM ALBUMIN

This project will study the encapsulation of bovine serum albumin (BSA) in liposomes. The reason that this protein is used to be encapsulated is because of its similarity to human serum albumin (HSA), a transport protein in human blood (13). Albumin is often used as drug carrier, because it has interesting properties. The protein is biodegradable, biocompatible, stable, has a low toxicity and no immunogenicity (14). The onset temperature for modifications in the structure of BSA is 58°C and the denaturation temperature is 62°C (73). The amino acid sequence of human albumin has a 76% similarity with the bovine one (61). BSA is a zwitterion and has an isoelectric point of 5.82, it is negatively charged at a pH of 7.4 (15). A BSA solution in ultrapure water at pH 6.1 has a mean zeta potential of -28.9mV. BSA consists of only one single polypeptide chain, has a helical structure and a molecular mass of 66.430kDa (74). Both proteins can bind and transport molecules such as metabolites, fatty acids, hormones, drugs in the blood. BSA as well as HSA contains 3 homologous domains in which each domain has two subdomains (A and B). Various drugs can be bound in domain III. BSA is an abundant protein and often used for research instead of HSA because of its stability. It turns out to be chemical inert in many biological and chemical reactions and it is

easy to purify. BSA shows unusual ligand binding properties, it can bind a tremendous amount of ligands in a reversible way. Another, economically important factor is its low cost. BSA is a protein of bovine blood, which is a by-product in the beef industry. BSA has the interesting property of undergoing reversible conformational changes when the pH is decreased in a range from 7 to 2. Because of the fact that BSA is a polyampholyte with a pH dependent charge, it provides reversible binding sites to load and release drugs in the body (13, 14).

1.3.1. Fluorescence

Various proteins show absorption in the near ultraviolet (UV) range. This is due to the presence of tryptophan, tyrosine and also, but less, due to phenylalanine and disulphide bonds (16). Both BSA and HSA are fluorescent, but they differ in their ability to emit light. HSA lacks the second intrinsic tryptophan residue at position 131, that BSA does have. The contribution of the abundant amino acid tyrosine in albumin molecules is minor to that of tryptophan and depends on the selected excitation wavelength (1). Tryptophan is an aromatic amino acid, this structure may contribute to the fact that tryptophan is able to exhibit fluorescence (75). Fluorescence emission spectra of proteins containing tryptophan can be used to examine changes in conformation, substrate binding and denaturation because of the high sensitivity of tryptophan to its local environment.

1.3.2. BSA and nanoparticles: history

Table 1.1 gives a brief situation of which nanoparticles with BSA have been developed before. Also the purpose and main achievements of these reported nanoparticles are shown.

A brief summary of previous research with BSA and nanoparticles

List of abbreviations:
[a] PEG = polyethylene glycol
[b] PLGA = Poly(lactic acid-co-glycolic acid)
[c] Folate-PEG-g-TMC = folate-poly(ethylene glycol)-grafted-trimethylchitosan
FITC = Fluorescein isothiocyanate
[d] GL-BSA-HCPT-NP = 10-hydroxycamptothecin-loaded glycyrrhizic acid-conjugated bovine serum albumin nanoparticles
[e] PCN = polyelectrolyte complex nanoparticle
[f] PPD/pDNA = poly(vinyl pyrrolidone)-graft-poly(2-dimethylaminoethyl methacrylate)/plasmid deoxyribonucleic acid
[g] MPA-capped-CdTe-QDs = mercaptopropionic acid – capped – cadmium telluride – quantum dots
[h] PEI = polyethylenimine
[i] NSP = nanoporous silicon particles

Table 1.1 A brief summary of previous research with BSA and nanoparticles

Nano-delivery system	Purpose	Main Achievements	Ref.
Reversible swelling-shrinking nanogel	– Quick release of encapsulated chemotherapeutics in cancer cells	– Efficient cytotoxicity	(17)
BSA-gel-capsules	– Study of the structure – Evaluate the pH-controlled release – Study of in vitro cytotoxicity – Study of *in vivo* antitumor property – Study to promote the development of polyelectrolyte microcapsules as drug delivery system	– pH-controlled loading and release – Effective accumulation in the lung – Doxorubicin-loaded BSA-gel-capsules induced apoptosis of B16-F10 cells + inhibited growth of pulmonary melanoma – Possibility to apply BSA-gel-capsules to drug delivery by IV injection	(18)
Nanosphere	– BSA as model drug for peptides	– Potential drug delivery system	(19)
Bilosomes	– Vehicle for oral mucosal immunisation with BSA as model antigen - Characterisation	– Size: 157±3nm PDI: 0.287±0.045nm zeta potential: -21.8±2.01mV entrapment efficiency: 71.3±4.3% – Sustained drug release up to 24h – In comparison with free antigen: - Higher in-vitro cell uptake in macrophage cells - Higher intestinal uptake - Higher systemic immune response – Induces mucosal and cell mediated immune response	(20)
BSA liposomes with PEG[a] (stealth agent modifier)	– Improve stealth and decrease clearance by macrophages	– Inclusion of 5% PEG: - Decrease of particle size and PDI - Zeta potential close to zero - Insufficient to reduce macrophage internalization – 10% PEG improves the stealth degree – PEGylated surfactant (5mg/mL) improves stealth of BSA NP's	(8)
BSA loaded gelatin microspheres	– High loading efficiency and low particle size	– Ability to prepare microspheres with: - High loading efficiency - Optimal size for uptake into gut-associated lymphoid tissues and systemic immunoresponsive organs	(21)

Nano-delivery system	Purpose	Main Achievements	Ref.
BSA-PLGA[b]-based core-shell NP	– Carrier system for water-soluble drugs (such as gemcitabine) – Preparation, optimization and *in vitro* evaluation	– Particle size: 243nm PDI 0.13 – Encapsulation efficiency: 40.5% – Drug loading: 8.5%w/w – Sustained release for 12 hours – Quick (2h) and efficient cellular uptake – Gemcitabine loaded core-shell NP: increased cytotoxicity against MG-63 cells (in comparison with marketed formulations)	(22)
Nano-scaled spherical polyelectrolyte complexes between the folate-PEG-g-TMC and FITC-BSA[c]	– Development of a receptor-mediated intracellular delivery vehicle	– Intracellular protein delivery vehicle with enhanced cellular uptake in cells which over-express folate receptors	(23)
FITC-BSA-loaded PEG modified lipoparticles and liposomes	– Development of alternative NP's to improve the stability	– Particle size: 133.7 ± 8.6nm – Zeta potential: + 13.3mV – Encapsulation efficiency: 59.7% – Release profile: first small burst released, afterwards continued and controlled release – In comparison with liposomes: - Protein retention is twice as long - Less cytotoxic and cellular uptake was more efficient	(24)
Chitosan-conjugated, pluronis-based nanogel	– Improve drug delivery of hydrophilic molecules across human skin – BSA is used as hydrophilic protein	– Transcutaneous permeability of hydrophilic proteins with different sizes (6-67kDA (BSA))	(25)
Drug-loaded chitosan-tripolyphosphate nanofibres	– Characterization of drug loading and *in vitro* release – BSA as high molecular-weight bioactive molecule model	– Sustained release in tissue engineering	(26)
BSA-loaded chitosan NP	– *In vitro* characterization – BSA is used as antigen	– Effective drug carrier and adjuvant for non-invasive, oral mucosal immunization – Simple, stable, painless, potentially safe and economical	(27)

Nano-delivery system	Purpose	Main Achievements	Ref.
GL-BSA-HCPT-NP[d]	– Characterisation of new type of BSA based drug delivery system with liver tumor targeting	– Particle size: 157.5nm – Zeta potential: -2.51 ± 0.78mV – Encapsulation efficiency: 93.7% – Drug loading efficiency: 10.9% – Release of drug is slow and continuous – Hemolysis testing: safety assured – Good targeting → Promising targeting delivery system for hepatocellular carcinoma therapy	(14)
Polysaccharides based PCN[e]	– Characterisation – BSA used as model drug	– Good stability – Encapsulation efficiency: up to 69% – Sustained release → promising drug delivery system with sustained release properties for hydrophilic bioactive molecules + long-term circulation in bloodstream	(28)
BSA-NP modified with lactoferrin, mPEG2000 and doxorubicin	– Study of blood brain barrier penetration and brain glioma cells targeting	– Promising drug delivery system for targeting of brain gliomas	(29)
BSA-NP	– BSA-NP loaded with vinblastine sulphate (VBLS) to obtain a tumor-specific drug carrier	– Particle size: 156.6nm – Entrapment efficiency: 84.83% – Drug loading efficiency: 42.37% → effective in targeting VBLS-sensitive tumours	(30)
Protein-polymer nano-vesicle	– Development of new biodegradable protein-polymer vesicle (BSA-PCL) and study of antitumor activity	– BSA-PCL linked to cetuximab: enhanced cell uptake – Doxorubicin encapsulated: enhanced antitumor activity compared to free doxorubicin → promising drug delivery vehicle in cancer therapy	(31)

Nano-delivery system	Purpose	Main Achievements	Ref.
BSA-loaded calcium-deficient hydroxyapatite nano-carriers.	– Development and study of controlled drug delivery system – BSA used as model protein	– Drug release is dependent on synthetic process and pH – Acid growth, acid protein-drug can be loaded – Release: – *Ex-situ* process: burst – *In-situ* process: initially burst + later: slow release	(32)
Folate-decorated ergone-BSA NP	– Improvement of therapeutic effect of ergosta-4,6,8(14),22-tetraen-3-one (ergone)	– Spherical shape, uniform size, zeta potential = -23.8mV – Drug loading content = 2.73% – Encapsulation efficiency = 61.8% – Slow drug release in blood stream – Increased drug release at target sites – Cell-killing activity: specific for cells that express the folate receptor (FR) → Potent activity against FR-positive tumors	(33)
Protein-coated Fe_3O_4 NP	– Novel technique for a minimal invasive elimination of solid tumours	– Stable, rapid heating and cell killing activity – BSA coating provides a platform for incorporating targeting molecules for targeted tumor thermal therapy	(34)
Nano-sized PPD/pDNA[f] complex	– Assemblage with BSA to screen the positive surface charge and reduce cytotoxicity	– BSA/PPD/pDNA showed no cytotoxicity + high gene transfection HepG2 cells	(35)
Bolaamphiphilic cationic vesicles with acetylcholine head groups	– *In vivo* and *in vitro* study for the ability to deliver BSA conjugated to fluorescein isothiocyanate across biological barriers	– Ability to deliver proteins across biological barriers, such as the cell membrane and the blood-brain barrier. – Brain cholinesterase activity destabilizes the vesicles: - release of the encapsulated protein - accumulation in the brain	(36)
BSA loaded biodegradable chitin nanogels with MPA-capped-CdTe-QDs[g]	– *In vitro* cellular localisation studies – Simultaneous drug delivery, bioimaging, and biosensing – BSA = model protein	– Nanogels can detect pH changes - pH-regulated protein release in abnormal pH of 5-7.4 (in pathological areas) - Improves therapeutic efficiency	(37)
Fe_3O_4 paramagnetic NP's modified with surface conjugation of PEI[h] BSA	– To disperse and stabilize oil in water emulsions containing coumarin-6 as the model drug	– Disease diagnosis and imaging guided drug release	(38)

Nano-delivery system	Purpose	Main Achievements	Ref.
Silk fibroin nanoparticles	– Sustained ocular drug delivery – BSA as macromolecular protein drug model	– Sustained release – Bioadhesive – Co-permeation – No damage to ocular tissue – Quick and sustained adhesion on outer scleral tissues + migration to interior	(39)
NSP[i]	– Surface modification of NSPs to preserve protein stability – BSA as probe protein	– Silicon particle as a protein carrier – Control of cell function – Preserves protein integrity during delivery	(40)
Cylindrical block copolymer nanochannels	– Long-term controlled protein drug delivery system – BSA = model drug	– Treatment of chronic diseases	(41)
BSA coated liposomes	– Surface modifications to prepare stealth liposomes with good bioavailability and good stability	– Anticancer drug carrier with long half-time – improved cellular uptake of liposomes loaded with anticancer drugs	(15)
Albumin or polyallylamine antibiotic-loaded nanoparticles in carboxylated polyurethane acid	– Delivery system for antibiotics to prevent medical device-related infections	– Antimicrobial effect up to nine days	(42)
BSA nanospheres coated with several fatty acids	– Use of thermally cross-linked BSA nanospheres coated with diverse fatty acids to control the release of vancomycin in the colon	– Drug release in the stomach is low – Satisfactory release in intestine – Good loading capacity, swelling tendency and mucoadhesion – Great potential in colon-specific delivery of peptidic drugs	(43)
PEG/bio-macromolecule nano-complexes in organic solvents	– Characterisation of size and morphology – Study of structural integrity – BSA as a protein macromolecule	– Stable nano-complexes (no aggregation nor precipitation) – Potential sustained release formulation for several therapeutic biological drugs	(44)
Polylactic polyglycolic acid (50:50) co-polymer	– Efficiency study between micro- and nanoparticles – BSA as a model protein	– Efficiency of uptake by intestinal tissue was much higher with nanoparticles than microparticles.	(45)

2. OBJECTIVE

For decades, liposomes have been used in site-specific drug delivery. Dioctadecyldimethylammonium bromide (DODAB) is a frequently used phospholipid to prepare cationic liposomes. DODAB:MO nanoparticles show a great potential to be used as a drug delivery system (70). Monoolein (MO) has the advantage to lower the net positive charge of the liposome, which decreases the transfection-associated cytotoxicity in gene therapy (50). Adding MO also lowers the high gel-to-liquid crystalline phase transition temperature of a DODAB liposome, which results in a better drug delivery system in the human body.

To ensure that DODAB:MO liposomes can be used as a nanoparticle system, they have to be characterised. A DODAB:MO ratio of (1:2) showed promising results in antigen immunization, drug delivery and gene therapy (50). It is important that the particle size is small enough to act as a non-immunogenic intravenously nano-delivery system with a long circulation time in the blood. Another essential element of the liposomes is their zeta potential, because this is directly related with the stability. The particle size and zeta potential were measured using respectively dynamic light scattering (DLS) and electrophoretic light scattering (ELS) techniques. To examine the stability of the liposomes, the particle size and zeta potential were measured every week and changes were evaluated.

Liposomes are not really beneficial if they show a poor encapsulation efficiency of drugs. When the entrapment is low, more drugs are needed to prepare a delivery system with enough therapeutic efficiency. Consequently, preparing drug entrapped liposomes will become more expensive. To overcome this problem, BSA is encapsulated in the DODAB:MO (1:2) particles in order to act as a drug carrier and facilitate the loading and releasing of drugs. The encapsulation efficiency was tested by measuring the BSA concentrations after centrifugation and separation of the BSA encapsulated in the lipid fraction from the BSA in the aqueous media that was not encapsulated. The incorporation of BSA in the liposomes was also evaluated by determination of BSA partition coefficient in the lipid/aqueous media.

To obtain a better view of the molecular structure of the DODAB:MO liposome and the secondary structure changes that might occur by BSA encapsulation, circular dichroism

measurements were carried out on blank liposomes and on liposomes hydrated with a BSA solution. The encapsulation/complexation process leads to particles in which BSA can be positioned inside the vesicle or attached to the outside surface of the liposome. To determine where exactly BSA is located, the zeta potential measurements were examined and compared with the results of the encapsulation efficiency assay.

3. MATERIALS AND METHODS

3.1. MATERIALS

Materials	Purchased from	City, Country
Ethanol for analysis 2-[4-(2 Hydroxyethyl)-1-piperazinyl]-ethanesulfonic acid or HEPES Acetic acid Sodium acetate crystalline GR	Merck KGaA	Darmstadt, Germany
Dioctadecyldimethylammonium bromide	Tokio Chemical Industry Co. (TCI)	Toshima, Japan
Monoolein (1-oleoyl-rac-glycerol) Chloroform Albumin from bovine serum Sodium hydroxide solution 50% in H_20	Sigma – Aldrich	St. Louis, MO
Nitrogen gas	Alphagaz™	Algés, Portugal
Nuclepore Track-Etch Membrane filters	Whatman	Kent, UK
Vortex Genie ™	Scientific industries, Inc.	New York, USA
Branson 1200 ultrasonix bath	Branson Ultrasonics	Danbury, USA
Memmert drying cabinet U40	Memmert	Schwabach, Germany
Warm Water Bath	VWR	Wayne, USA
Lipex Extruder	Northern Lipids Inc.	Burnaby, Canada
Ultrapure water by Milli-Q synthesis equipment	Millipore Corporations	Massachusetts, USA
Analytical balance	Denver Instrument	New York, USA
Disposable polystyrene cuvettes of 10x10x45mm non-pyrogenic sterile-R-filter (0.2µm and 0.45µm)	Sarstedt AG&Co	Nümbrecht, Germany
Disposable folded capillary cell (zeta potential) Malvern Zetasizer Nano ZS analyser	Malvern Instruments Ltd	Worcestershire, UK
UV-3101PC UV-VIS-NIR scanning spectrophotometer	Shimadzu Corporation	Tokyo, Japan
Quartz cuvettes	Hellma Analytics	Müllheim, Germany
Perkin Elmer Luminescence Spectrometer LS 50	Perkin Elmer	Waltham, MA
Amicon ultracel®-50K and 100K centrifugal filter units (100 000 MWCO)	Merck Millipore Ireland Ltd	Tullagreen, Ireland
centrifuge 5804 R	Eppendorf	New York, USA
691 pH meter	Metrohm	Herisau, Switzerland
J.A.S.C.O. J-815 CD spectropolarimeter	Jasco Analytical Instruments	Easton, USA

3.2. LIPOSOME PREPARATION

3.2.1. General liposome preparation – hydration technique

Currently, the most common technique to reduce the liposomal size is extrusion. The disadvantages of this method are the decrease in encapsulation efficiency and the possibility to change the structure of asymmetric liposomes. Also, in order to obtain the desired low particle size, it is recommended to carry out more than ten extrusion cycles through a membrane with a pore size less than 200nm (7).

The following method can be used to prepare liposomes with all kinds of lipids. However, the characteristics of the final liposomes can differ depending on which kind is used. Liposome preparation starts by making a lipid film in a glass flask. If more than one lipid is used (such as a combination of DODAB and MO), then the ethanolic lipid solutions have to be mixed with an organic solvent such as chloroform. This is necessary to obtain a homogeneous mixture. The solvent, containing chloroform and ethanol, is evaporated using a dry nitrogen stream in a fume hood. After drying, lipid films can be stored in a freezer.

To loosen up the lipids from the glass flask a hydration procedure is carried out. This process is simply adding an aqueous medium to the dry lipid film. This medium should contain the chemicals that have to be encapsulated in the liposomes. The temperature of the hydration medium should be at a temperature above the T_m of the lipid with the highest T_m. Though, when proteins are used, the temperature should not be above the denaturation temperature of the protein. Vigorously shaking and stirring for one hour above the T_m for the whole hydration procedure is highly recommended. After the hydration procedure, multilamellar vesicles (MLV) are formed.

Next, lipid extrusion is carried out on the lipid suspension. Dependent on the desired particle size, the extrusion will be done in several cycles using filters of a different pore size. The use of filters with larger pore size first, followed by smaller ones is necessary to obtain a suspension with a homogenous size distribution. This order of filters also prevents the lipid membranes from fouling. The extrusion also has to be done at a temperature above the highest T_m of the used lipids. A pressure of 4-8mbar can be used. After the extrusion process, the samples should be stored in a fridge until they can be further analysed (76, 77).

3.2.1.1. Overnight aging

It is believed that aging of the MLV overnight with a temperature above the T_m, would facilitate the extrusion and improve the homogeneity of the size distribution, which lowers the polydispersity index (3.3.1).

3.2.2. Preparation of DODAB:MO (1:2) liposomes – hydration technique

To prepare the liposomes for this project, a stock solution of DODAB and MO was needed. A 20mM ethanolic solution of DODAB was made by weighing 126.2mg of DODAB and dissolving it in ethanol to a volume up to 10.00mL in a volumetric flask. A 20mM ethanolic solution of MO was made by weighing 71.3mg MO and dissolving it in a volumetric flask up to 10.00mL with ethanol.

Glass tubes were cleaned with ethanol and dried in a drying oven. DODAB:MO (1:2) lipid films with different molar concentration of lipids were made by pipetting different volumes of DODAB and MO into glass tubes (Table 3.1). After collecting DODAB and MO in a (1:2) ratio, chloroform was added and the solvent (consisting of ethanol and chloroform) was dried under a nitrogen stream with a constantly rotating motion. After the evaporation, the lipid films were stored in a freezer at -10°C. Later, the frozen lipid films were hydrated with a BSA solution. Different BSA/lipid ratios, were prepared according to Table 3.1. All samples were prepared in triplicate.

Table 3.1 Volumes of DODAB, MO, BSA stock solutions used to prepare LUV with different BSA/lipid ratios

volume DODAB (20mM) (µL)	volume MO (20mM) (µL)	volume BSA in ultra -pure water (mL)	BSA concentration used (mg/mL)	[lipid] (mM)	BSA/lipid molar fraction χ
83.3	166.7	10.0	0.1[a]	0.5	0.752
83.3	166.7	12.5	0.2	0.4	0.883
83.3	166.7	25.0	0.2	0.2	0.938
41.7	83.3	25.0	0.2	0.1	0.968
16.7	33.3	25.0	0.2	0.04	0.987

[a] **By reducing the BSA stock concentration in this sample it was possible to reach the same BSA/lipid ratio without increasing the lipid concentration to 1mM which was extremely difficult to extrude.**

The hydration medium (BSA stock solution) was warmed up above the T_m (45°C). However, care was taken not to increase the temperature above 58°C, because this is the

onset temperature at which the BSA protein structure starts to change due to denaturation (73). A cycle of one to two minutes of incubation in a warm water bath at 50.0°C and one to two minutes vigorously vortexing was repeated, for at least one hour until the whole lipid film was removed from the glass container. Whenever needed, the sample was sonicated for 30 seconds to help removing the lipid film. This entire process created MLV. Subsequently, the vesicles were extruded five times through a polycarbonate filter with a pore size of 0.4µm using a Northern Lipids Lipex Extruder and Nuclepore Track-Etch Membrane filters. After the extrusion process, LUV with the desired size were formed. The samples were stored in a fridge at a temperature of 6°C until the analysis by Malvern Zetasizer Nano ZS particle analyser.

3.2.2.1. Overnight aging

Because of the limited stability of LUV, the liposome preparation was done several times during this project. The MLV and LUV preparation were usually carried out in the same day. An overnight aging procedure was tested to study the effect on the particle size and stability of this particular liposomal formulation. In this case, MLV preparation by the lipid film formation and hydration technique was carried out and the samples were kept overnight at a temperature of 50.0°C. The next day, the MLV were extruded to obtain the aged LUV formulation.

3.2.2.2. Liposomes prepared with different extrusion cycles

Two liposomes suspensions with a BSA/lipid mole ratio of 0.968 were prepared with the overnight aging procedure (as described in 3.2.1.1) were extruded in two different ways. Also two liposome suspensions with a BSA/lipid mole fraction of 0.987 were prepared, but this time without aging (as described in 3.2.2). From both BSA/lipid mole ratios one sample had five extrusion cycles through a membrane with a pore size of 400nm. The other sample was prepared in the same way, but was afterwards also extruded five times through a 200nm pore sized filter.

3.3. LIPOSOMAL CHARACTERISATION BY DLS AND ELS

3.3.1. Mean diameter and polydispersity index (PDI)

Particles in a solution are subjected to the Brownian motion. This is the random movement of particles in a fluid, which is a result of collisions with solvent molecules that surround them. The speed of those movements is used to determine the particle size by Dynamic Light Scattering (DLS) methods. The principle of DLS is based on the fact that an incident beam source illuminates the sample and the movement of particles causes scattering of light. It is possible to establish a correlation between the size of the particles and the scattering vector intensity, because small particles diffuse faster in a liquid than bigger particles (63).

A volume of 1mL of each sample was placed in a 3mL disposable polystyrene cuvette. The mean diameter (d.nm), its respective standard deviation (d.nm) and the polydispersity index (PDI) were measured by means of DLS in a Malvern Zetasizer Nano ZS particle analyser. Three independent measurements of ten runs each were carried out with the parameters shown in Table 3.2.

Table 3.2 Parameters used to measure the particle size with a Malvern Zetasizer Nano ZS particle analyser.

Material	Polystyrene latex
Refractive index	1.590
Absorption	0.01
Dispersant	Water
Temperature	°C
Viscosity	0.8872cP
Refractive index	1.330
Dispersant viscosity is used as sample viscosity	
Temperature	25.0
Equilibration time	120 seconds
Cell type	DTSOO12 – Disposable sizing cuvette
Angle of detection	
Measurement angle	173° Backscatter (NIBS default)
Measurement	
Number of runs	10
Run duration	10 seconds
Number of measurements	3
Delay between measurements	0 seconds
Positioning method	Seek for optimum position
Automatic attenuation selection	Yes
Analysis model	General purpose (normal resolution)

The PDI is related to the peak width of the size distribution graph and consequently shows if the nanoparticle suspension is mono- or polydisperse. The more homogeneous the size distribution is, the lower the PDI will be. The values for having a mono- or polydisperse distribution are not consensual. It is generally accepted that an ideal unimodal distribution should have a PDI below 0.02. When the nanoparticle suspension is almost monodisperse, PDI values of 0.02 to 0.08 are found. Above 0.08, it is said that the particles are polydisperse. When rigid particles are measured, it is appropriate to target these values. However, when softer materials (such as liposomes) are used, reaching those values is much more difficult. In this particular case, where a mixture of two lipids and a protein is used, it is even more difficult to reach a very low PDI. However, values of 0.2 were considered as acceptable for a fairly homogeneous size distribution.

When particle size is measured by DLS, the result will be given as an intensity particle size distribution (PSD) and these are also the results that are presented in this paper. However, the number distribution was also considered whenever an intensity population with distinct sizes was observed. By the analysis of the number distribution it was possible to elucidate the relative percentage of each population.

3.3.2. Superficial charge density (ζ-potential)

A liquid usually contains ions which are attracted to the surface of suspended particles, but only if they have an opposite charge. The net charge of the particle determines the distribution of the counter ions. The binding strength depends on the distance of the counter ions to the suspended particle. The liquid layer in which the counter ions are strongly bound is called the Stern layer. Loosely bound ions form the Diffuse Layer. Within this layer there is a notional boundary called the Slipping plane. Ions beyond the Slipping plane will keep their own position if the charged particle moves in the liquid. Ions within the boundary will move with the particle. The zeta potential (ζ-potential) is the potential measured at the Slipping Plane. The ζ-potential is measured by means of Electrophoretic Light Scattering (ELS) and Laser Doppler Velocimetry. An electrical field is applied and the velocity of the charged particle in the liquid is measured. The ζ-potential is then calculated using the velocity, viscosity and dielectric constant (63).

For ζ-potential measurements, a clear disposable folded capillary zeta cell was filled with 1mL of each sample and placed in a Malvern Zetasizer Nano ZS analyser. Three independent measurements of 25 runs were carried out. The ζ-potential was measured every week until the end of the project. The ζ-potential gives information about the liposome surface charge, which cannot be measured directly. The liposome surface charge determines the tendency of suspended particles in a liquid to flocculate, thus it gives a measure of the formulation shelf stability. The lower the modulus of the zeta potential, the less the particles repel each other, the easier flocculation or aggregation occurs and the less stable and useful the particles are (63).

Table 3.3 Parameters used to measure the zeta potential with a Malvern Zetasizer Nano ZS particle analyser.

Material	Polystyrene latex
Refractive index	1.590
Absorption	0.01
Dispersant	Water
Temperature	°C
Viscosity	0.8872cP
Refractive index	1.330
Dielectric constant	78.5
F(Ka) selection	Smoluchowski
F(Ka) value	1.50
Dispersant viscosity is used as sample viscosity	
Temperature	25.0
Equilibration time	120 seconds
Cell type	DTS1060C – Clear disposable zeta cell
Measurement	
Number of runs	25
Number of measurements	3
Delay between measurements	0 seconds
Automatic attenuation selection	Yes
Automatic voltage selection	Yes
Analysis model	Auto mode[a]

3.4. DETERMINATION OF BSA ENCAPSULATION EFFICIENCY

3.4.1. BSA calibration curve

To quantify the amount of BSA that is encapsulated after the hydration and extrusion process, UV-visible spectrophotometry and fluorescence were used. In order to determine the BSA molar absorptivity, an UV-visible and fluorescence calibration curve in ultrapure water was made.

A stock solution of 1mg/mL BSA in ultrapure water was made. All other samples, with BSA concentrations of 0.05, 0.1, 0.2, 0.3, 0.4, 0.5, 0.6, 0.7, 0.8, 0.9mg/mL were prepared by rigorous diluting the stock solution.

3.4.1.1. Ultraviolet-visible spectrophotometry

UV-visible absorbance of each sample was measured between 250nm and 320nm. To reduce the signal/noise ratio, the scan speed was set on 'slow' and the slit width was set to 2.0nm. The absorbance was read at a temperature of 37.0°C.

3.4.1.2. Fluorescence

This technique was also used for BSA quantification as it is much more sensitive than UV-visible spectrophotometry, thus it is possible to extend the linearity of the Beer Law to smaller concentrations.

Before fluorescence was used to determine the BSA concentration, it had to be proven that BSA emits light upon excitation. This can be done by means of reading the emission of a sample at three different excitation wavelengths. The first one was the emission wavelength where the maximum excitation is found. The excitation of the two others was measured at an emission wavelength preferably close to the one where the maximum excitation is found. If only the intensity, but not the wavelength changes with the use of a different emission wavelength, then it can be concluded that BSA effectively excites light and has fluorescent characteristics. The maximum excitation is found at an emission wavelength of 274.00nm. The excitation is read at 274.0nm, 265.0nm and 280.0nm.

First, a broad emission and excitation scan was carried out in order to set up the correct parameters. The emission was read from 300nm to 500nm. The excitation wavelength was chosen according to the wavelength of maximal UV-absorbance.

BSA was excited through a group of consecutive wavelengths from 200nm till 300nm in which the emission wavelength was the one that produced the maximum fluorescence emission.

Both emission and excitation of BSA in ultrapure water were read in a Perkin-Elmer LS 50 fluorimeter at a room temperature (21°C) and at 37.0°C. The slits were set to 12.0nm and the scan speed was set to 500nm.

3.4.2. Amicon Ultra-Centrifugation

Liposomes were prepared with a known amount of BSA in the hydration medium. In an ideal situation all BSA would be encapsulated in the liposomes. However, some of the initial BSA is lost on the polycarbonate filter during extrusion and some of the free BSA will not get encapsulated by the liposomes. To determine the amount of BSA that is held by the lipid vesicles (either distributed on the liposomal surface or enclosed within the liposomes), an encapsulation efficiency assay is carried out. The samples are centrifuged, using Amicon Ultra-15 Centrifugal filters of 100KDa. The BSA can pass the filter while the liposomes cannot. Therefore, this process separates the BSA that is not encapsulated (filtrate) from the BSA encapsulated in the liposomes and retains on the filter (pellet).

First, the Amicon filters were thoroughly rinsed out by addition of 2mL of ultrapure water followed by centrifugation during 15 minutes at 4000rpm and at a temperature of 20°C. This procedure was done twice to assure that the filter units were cleaned. After the washing procedure, the water was discarded. The centrifuge tube and filter device, were dried with a tissue and the amicons were centrifuged upside-down to take out as much water from the filter as possible. Then, the Amicon® Ultra-15 device was refilled with 1.5mL of each sample. There were also two control samples consisting of only nanoparticles without any BSA incorporated and one sample of an aqueous BSA solution without nanoparticles. These control samples allow to test if respectively the nanoparticles and BSA pass through the filter. The centrifugation is carried out at 4000rpm and a temperature of 20°C. Every 15 minutes the centrifuge tubes were checked to see whether the sample was still passing through the filter or not. The samples were centrifuged until there was no change in the volume of the filtrate. When finished, both the filtrate and pellet were recovered and the volumes were written down and transferred into microcentrifuge tubes. Both filtrate and pellet were diluted up to 1.5mL with ultrapure water. The BSA concentration of the diluted filtrates and pellets was determined by means of UV-VIS

spectroscopy and fluorescence. Because the dilution was made with the addition of ultrapure water, the same parameters can be used as mentioned in 3.4.1.

The encapsulation efficiency is given by equation (3.1) and the BSA loading efficiency can be calculated using equation (3.2).

$$Encapsulation\ efficiency\ (\%) = \frac{[BSA]_{lipid}}{[BSA]_{total}} \cdot 100 \quad (3.1)$$

$$Loading\ efficiency\ (\%) = \frac{[BSA]_{incorporated}}{[BSA]_{initial}} \cdot 100 \quad (3.2)$$

In which: $[BSA]_{lipid}$ = the amount of BSA quantified in the lipid pellet (mg/mL)
= $[BSA]_{incorporated}$

$[BSA]_{total}$ = the total amount of BSA that is present after the extrusion process (mg/mL)
= $[BSA]_{filtrate} + [BSA]_{lipid}$

$[BSA]_{initial}$ = the amount of BSA in the hydration medium and added to the lipid film (mg/mL)

Preferably this study is carried out in the same day of production of the liposomes and then some weeks after to have some information about the shelf stability of the formulations

3.5. CIRCULAR DICHROISM

The biological function of a protein depends on its three-dimensional structure (tertiary structure) which is determined by its amino acid sequence (primary structure) and the cellular environment surrounding the polypeptide chain. The secondary structures are regular elements of a protein structure and consist of α-helices, β-strands and β-turns (64). The unordered arrangements as well as structures that cannot be classified within the standard classes are known as random coil conformation.

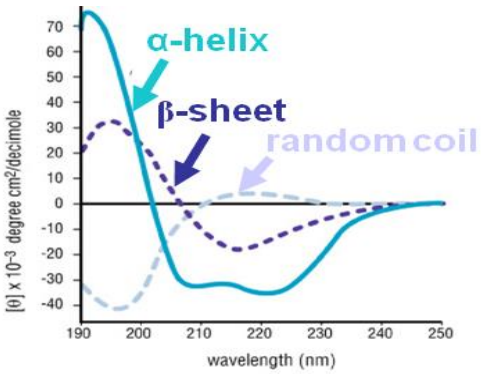

Figure 3.1 CD spectra of different peptide secondary structure

The secondary structure of peptides and proteins can be determined by circular dichroism spectroscopy (CD) in the far-UV spectral region. The technique is nondestructive, requires small amount of material and can be used for molecules in solution. CD is a chiroptical phenomenon by which optically active molecules such as proteins are able to interact with circularly polarized light. From this interaction results a characteristic CD spectrum according to their secondary structure. An example is shown in Figure 3.1 .

Protein misfolding is an alteration of the secondary or tertiary structure that results in malfunction. Misfolded proteins are particularly prone to aggregation because hydrophobic residues that are normally buried are exposed on their surfaces. Therefore, in the process of developing a nanoparticle with BSA it was important to assure that the protein kept its secondary structure, so that there was no aggregation or loss of capacity of protein binding. In order to know if BSA secondary structure has changed upon binding with the DODAB:MO liposomes CD spectra were recorded with a Jasco 815 spectropolarimeter from 190nm to 260nm using quartz cuvettes with an optical path length of 10mm.

3.6. DETERMINATION OF BSA PARTITION COEFFICIENT

Liposomes are able to carry hydrophilic, hydrophobic and amphiphilic molecules because of their biphasic properties. Depending on their coefficient partition molecules are located in different parts of the liposomes. Hydrophilic molecules are entrapped either in the inside aqueous phase or they are attached to the polar surface of the liposomes where they are in contact with the external aqueous environment. Lipophilic molecules on the other hand will be completely encapsulated within the lipid bilayer.

For most of the cases, the partition coefficient of a molecule between a lipid and an aqueous phase can be evaluated by UV-VIS spectrophotometry as long as there is a difference in an absorbance parameter of the partitioning molecule (e.g. molar absorptivity, ε, and/or wavelength of maximum absorbance, λ_{max}) when it is either in aqueous solution or after incorporation in the membrane (65). The difference in the wavelength of maximum absorption in the presence of liposomes in relation to the absorption maximum in buffer solution can also provide information about the distribution of the molecule between the aqueous and lipid phase. Indeed, bathochromic deviations (λ_{max} deviation to longer wavelengths) are indicative of a decrease in polarity in the molecule's surroundings and indicate an incorporation of the investigated compounds into the hydrophobic part of lipid bilayer. Hypsochromic deviations (λ_{max} deviations to shorter wavelengths) are indicative of the presence of the molecule in a more polar microenvironment (65).

Given the definition of the partition coefficient and the conditions under which the law of Lambert-Beer is applied, the absorbance of a solution containing a certain concentration of drug (Abs), that is distributed between the lipid (l) and aqueous (w) phase, can be related with K_p according to Equation 3.3 (65):

$$Abs_T = Abs_w + \frac{(Abs_l - Abs_w)K_p[L]V_\varphi}{1 + K_p[L]V_\varphi} \qquad (3.3)$$

In which:
Abs_T = total absorbance of the compound
Abs_w = aqueous absorbance of the compound
Abs_l = lipid absorbance of the compound
K_p = partition coefficient (dimensionless)
$[L]$ = lipid concentration ($mol \cdot L^{-1}$)
V_φ = lipid molar volume ($L \cdot mol^{-1}$).

Despite the apparent simplicity of Equation (3.3), its application is limited to systems with low scattering of light, such as micellar/aqueous systems. However, the presence of microstructures of heterogeneous sizes causes light scattering (65), particularly at wavelengths below 300nm. This results in a decrease of light that reaches the detector. The spectroscopic interference of light scattering, and the absorbance produced by the microstructures, will turn the analysis of changes in the absorbance of the molecule upon

partition into a difficult task. To eliminate the background signal intensity caused by the vesicles, the absorption spectra of vesicle suspensions with the same lipid concentration as the samples are measured. These spectra are subtracted from the correspondent sample spectra. Even if the suspensions in the samples and references contain the same amount of lipid vesicles, the counterbalance of the sample and reference beams is always incomplete. This obstructs the complete neutralisation of the strong background signals in order to obtain a flat and zero-level base line. The problem of the background interference of the medium due to light scattering of the vesicles is only eliminated by the use of derivative spectrophotometry (in order to the wavelength λ). In this context, the derivative spectrophotometry for the calculation of K_p is advantageous because it allows the elimination of interference caused by organized systems (difficult to cancel in zero-order spectrophotometry), without the need to employ techniques of phase separation. Furthermore, the derivative analysis of the spectra leads to a better resolution of overlapping bands (65).

The calculation of K_p by derivative spectrophotometry is based on an equation similar to Equation (3.3) (65):

$$D = D_w + \frac{(D_l - D_w)K_p[L]V_\varphi}{1 + K_p[L]V_\varphi} \quad (3.4)$$

In which: $$D = \frac{\partial^n Abs}{\partial \lambda^n} \quad (3.5)$$

The partition coefficients are then calculated by fitting Equation (3.4) to experimental derivative spectrophotometric data (D versus [L]) through a nonlinear regression method where the adjustable parameters are D_l and K_p.

Amphiphilic molecules, such as BSA can be either adsorbed onto the surface, entrapped in the aqueous environment or within the lipid bilayers. The determination of the K_p of BSA will complete the information gathered by the encapsulation and ζ-potential regarding the interaction of BSA with the liposomes NP. Partition coefficients of BSA were determined in LUV of DODAB:MO (1:2). BSA was added to liposomes containing a fixed concentration of BSA (0.1mg/mL and 0.2mg/mL) and increasing concentrations of lipids (in the range of 0.04–0.5mM). The correspondent reference solutions were identically prepared

in the absence of BSA. The absorption spectra of samples and reference solutions were recorded with a Shimadzu UV-3101PC UV-VIS-NIR Spectrophotometer using quartz cells with 10mm path length, in the 200–400nm range. After measurements the spectrum for the reference was subtracted from that of the sample to obtain corrected absorption spectra. Derivative spectra were calculated using the Savitzky–Golay method (65) in which a second-order polynomial convolution of 13 points was employed.

3.7. CONTROLLED RELEASE ASSAYS

In order to know the amount of BSA that is released from the liposomes during its stay in the human body, controlled release assays are carried out. The release of BSA will be different in each body fluid, because of the pH dependency of liposomes. Most important compartments in the human body for liposomal drug release in this project are the gastro intestinal track and human blood. To understand the release in these body fluids, calibration curves have to be made in an HEPES buffer and an acetate buffer to recreate respectively the pH of human blood (7.4) and the pH of the gastro intestinal track (5.0). A third solvent, ultrapure water has a pH of 6.1.

A stock solution of 1mg/mL BSA is made in each buffer solution. All other samples, with BSA concentrations of 0.05, 0.1, 0.2, 0.3, 0.4, 0.5, 0.6, 0.7, 0.8, 0.9mg/mL are prepared out of the stock solutions. A 10mM aqueous solution of HEPES is made. Therefore 595.75mg was weighted and dissolved in ultrapure water up to a volume of 250.00mL.

To prepare the acetate buffer a solution of acetic acid and sodium acetate was mixed. 2.89mL of acetic acid solution was dissolved up to 250.00mL with ultrapure water. 8.20343g sodium acetate was dissolved in ultrapure water and the volumetric flask was filled up to 500.00mL. 148.0mL acetic acid solution was mixed with 352.0mL sodium acetate solution and completed to a volume of 1000.00mL. The desired pH is respectively 7.4 and 5.0, which was controlled and adjusted by means of a pH meter and NaOH. Both buffer solutions were filtered through a non-pyrogenic sterile-R-filter of 0.2µm.

It has already been written in this report that the amount of BSA can be characterised by means of UV-visible spectrophotometry and fluorescence. The exact same parameters as mentioned under 3.4.1 will be used to read the fluorescence and UV-absorbance of each sample.

4. RESULTS

4.1. LIPOSOMAL CHARACTERISATION BY DLS AND ELS

4.1.1. BSA in ultrapure water solution

Three measurements of a 0.2mg/mL BSA in ultrapure water solution were made. The mean zeta potential amounts to -27.0 ± 12.3mV. The mobility did not decrease, which means that the temperature was stable during the measurements. Also three measurements of a 0.1mg/mL BSA in ultrapure water solution were made. The mean zeta potential of the BSA particles in the solution amounts to -30.8 ± 15.4mV. Also in this case, the mobility did not decrease. Both solutions had a pH around 6.1.

4.1.2. DODAB:MO (1:2) liposomes (encapsulated with BSA)

4.1.2.1. Particle size and PDI

The particle size and PDI of the liposomes were measured immediately after their extrusion. From the samples with a BSA/lipid molar ratio of 0.752 and 0.883 only two aliquots were made, because of the limited volume. All the other samples had three aliquots. The mean size for each sample plus the standard deviation and PDI are shown in Figure 4.1.

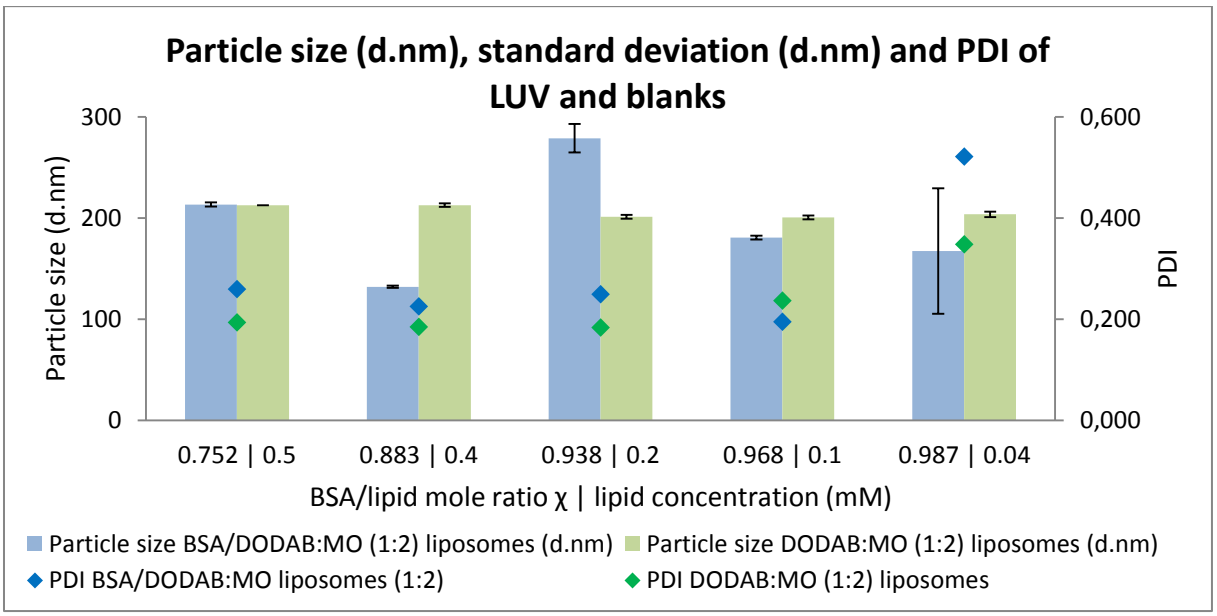

Figure 4.1 Mean particle size (d.nm) for each BSA/lipid molar ratio with its corresponding standard deviation (d.nm) and PDI.

The DODAB:MO (1:2) liposomes encapsulated with BSA are represented in blue bars. The blank DODAB:MO (1:2) liposomes are shown in green bars. The y-axis on the left indicates the particle size (d.nm) and on the right y-axis the polydispersity index is shown. the x-axis displays the BSA/lipid molar ratio χ in case of the BSA encapsulated liposomes or the lipid concentration (mM) for the blank liposomes. The samples were read immediately after the preparation of the liposomes.

All samples show values which correspond to only one size population except for the samples with higher liposome concentrations. In the sample with a mole fraction of 0.938 the mean size value is 279nm. The first aliquot shows a small percentage (2.7%) of aggregates. This increases the PDI from 0.232 (mean of only the two aliquots without any aggregates) to 0.332. In the 0.987 samples, the intensity distribution gives mainly two peaks correspondent to two populations of particles with different sizes: a small peak which corresponds to free BSA (with 7 nm), a bigger one that has an equivalent size to liposomes containing BSA (Figure 4.2).

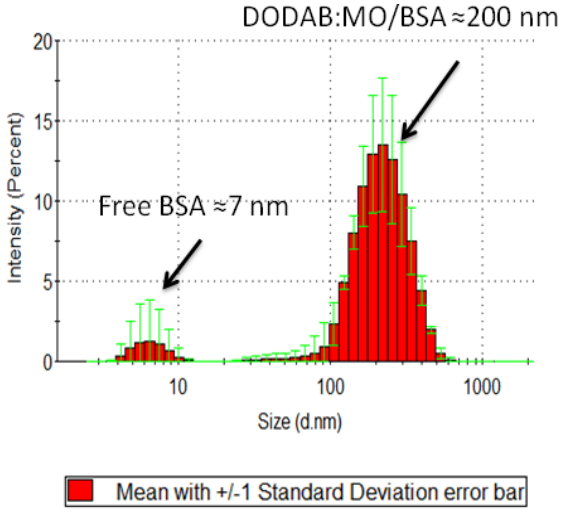

Figure 4.2 Size intensity distribution of BSA and BSA encapsulated in DODAB:MO (1:2) liposomes obtained for BSA/lipid mole fraction of 0.987.

The presence of different particle sizes distribution causes the elevated PDI. However, the number distribution shows a frequency of 100% of the smallest peak, indicating that the majority of the particles presented in this sample correspond to BSA aggregates.

A small particle size is desired. The liposomes with a BSA/lipid mole fraction of 0.883 have a PDI of 0.225 and the ones with a mole fraction of 0.968 have a PDI of 0.194, therefore they seem superior. Normally the PDI should be below 0.2, so it can be concluded that the liposomes in the solution have a polydisperse size distribution.

4.1.2.2. Zeta potential

Because of the limited volume, the samples with a BSA/lipid molar ration of 0.752 and 0.833 only had two aliquots. From the other samples, three aliquots were made. The mean zeta-potential for each sample plus de standard deviation are shown in Figure 4.3.

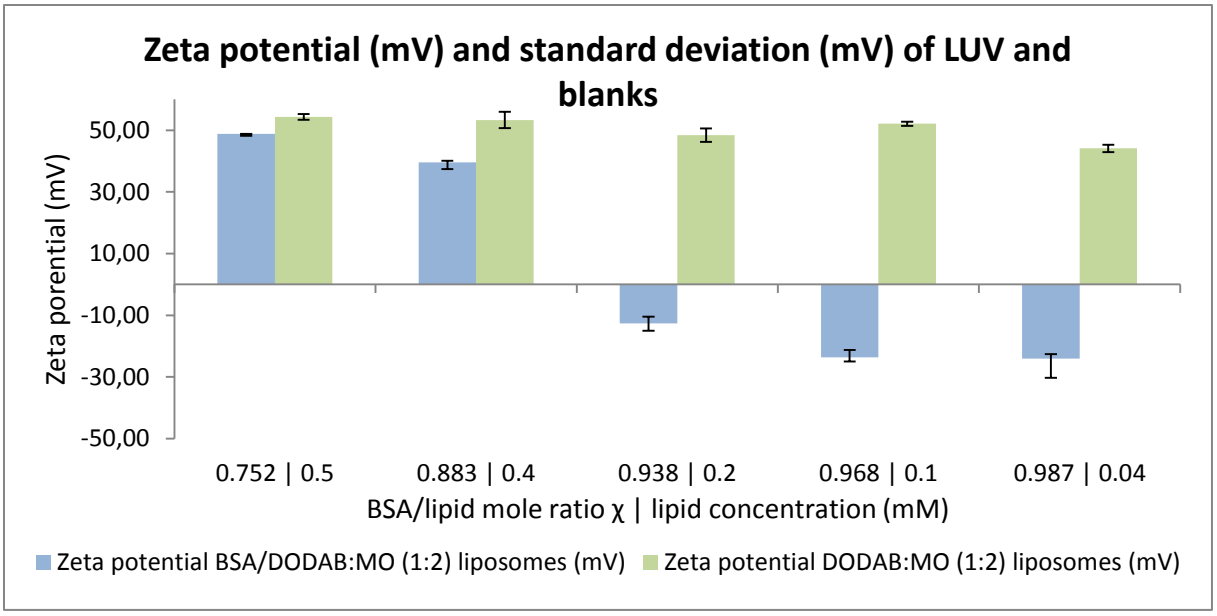

Figure 4.3 Mean zeta potential (mV) for each BSA/lipid molar ratio, with its standard deviation (mV). The samples were read immediately after preparing the liposomes. The DODAB:MO (1:2) liposomes encapsulated with BSA are shown in blue. The blank DODAB:MO (1:2) liposomes are shown in green. The y-axis describes the zeta potential (mV), the x-axis gives the BSA/lipid molar ratio χ in case of the BSA encapsulated liposomes or the lipid concentration (mM) for the blank liposomes.

DODAB:MO (1:2) liposomes hydrated with only ultrapure water have a mean zeta potential of +50.5mV (Figure 4.2) at a mean pH value ± standard deviation of 5.5±0.3, which is consistent with other reported values for the same type of liposomes (70). The liposomes encapsulated with BSA have a mean pH of 5.8 with a standard deviation of 0.2. The zeta-potential results (Figure 4.3) showed the progressive neutralization of the initial positive zeta potential of the DODAB:MO (1:2) liposomes with an increase in BSA concentration (which has a zeta potential of -28.9mV). At BSA/lipid molar fraction ratio of 0.938, the isoelectric point was reached, indicating that all negative charge from the BSA backbone has been neutralized by the addition of DODAB:MO (1:2) cationic vesicles. Liposomes with the lowest BSA/lipid molar ratios (0.752 and 0.883) are positively charged at their surface. This means that BSA is encapsulated inside of the liposomes and not adsorbed to the surface of the liposomes. However, in the case of BSA/lipid molar ratio of 0.883, there is already some observable reduction of the zeta-potential (from +50.5mV to +39.6mV) revealing some adsortion of BSA to the surface of the liposomes. Those two liposome suspensions are considered as stable immediatly after their preparation. Also all the blank DODAB:MO (1:2) formulations show a high stability. The the word ‘stability’ or ‘stable’ is used to indicate that the particles will not have any intention to aggregate as long as the surface potential remains unchanged.

4.1.2.3. Stability

To test the stability of the liposomes the particle size and zeta potential were measured every 8 days during 4 weeks and afterwards every 15 days until the end of the project.

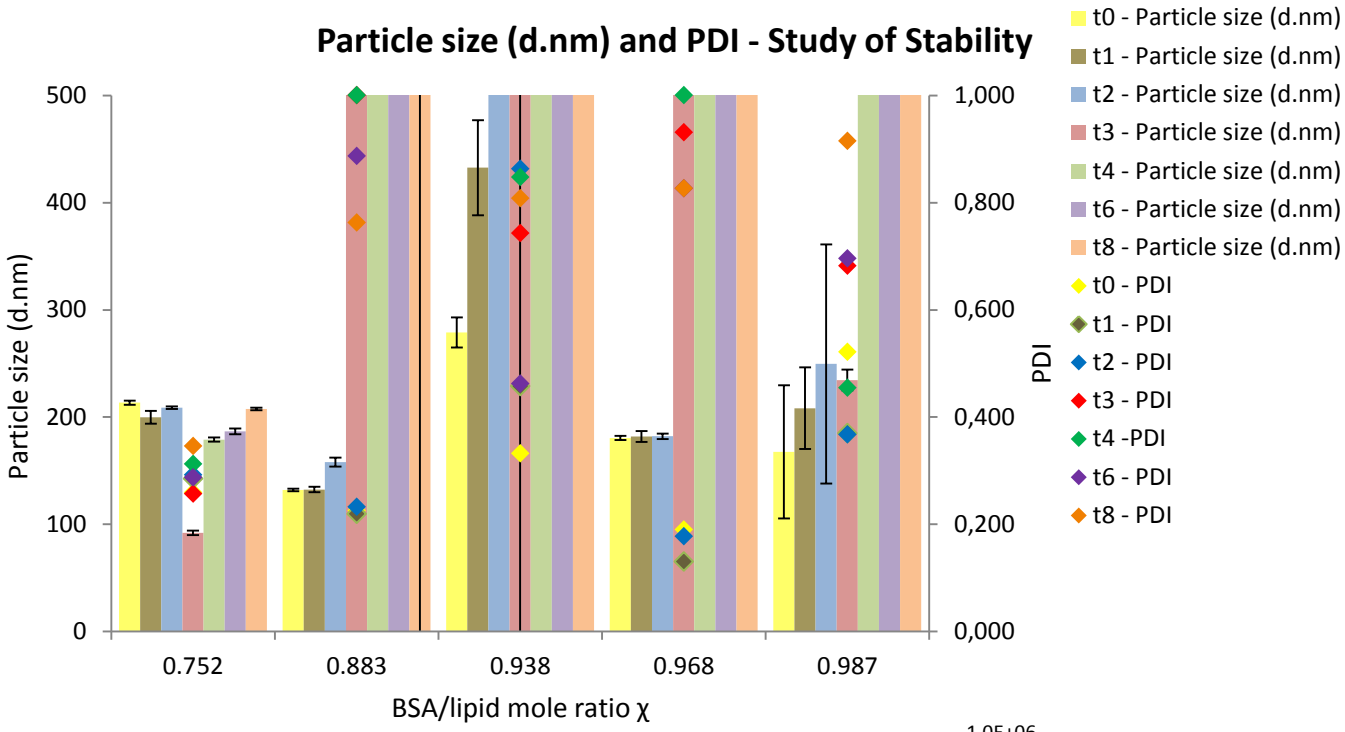

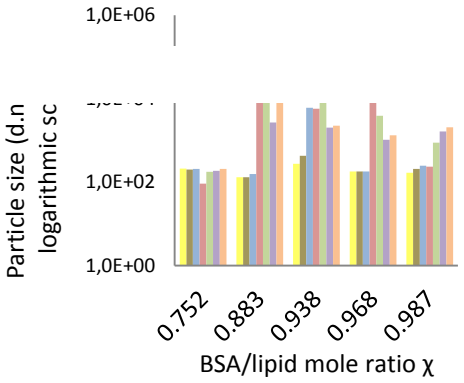

Figure 4.4 Stability study of the liposomes – Particle size and PDI. PDI, particle size (d.nm) and the standard deviations (d.nm) are shown for each BSA/lipid mole fraction
t_0 indicates the first time the particle size and PDI were read, which was immediately after the liposome preparation. The measurements read when the samples were one week old are indicated by t_1, two weeks old by t_2 and so on. Some values are cut off to make the graph more distinct. The particle size (d.nm) for each BSA/lipid mole ratio is represented in next graph. Note that the y-axis is represented in a logarithmic scale

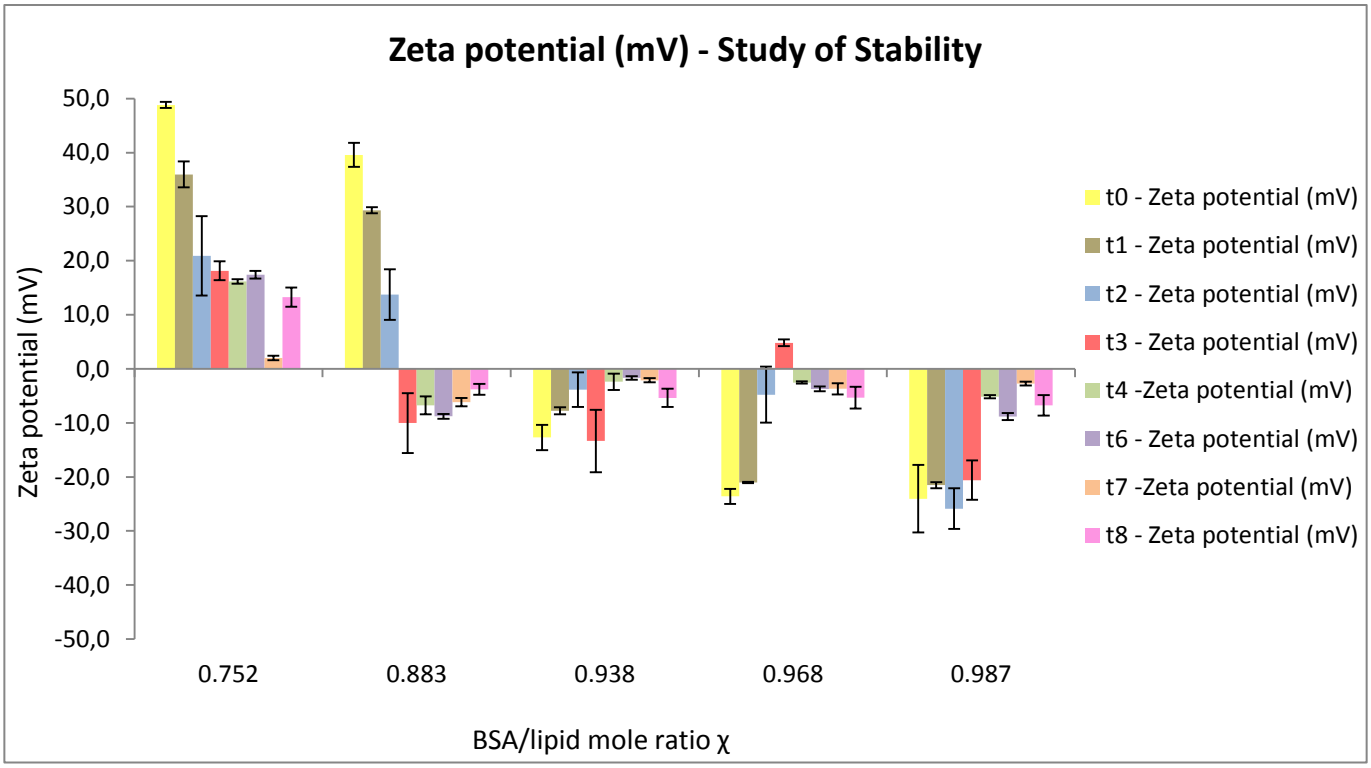

Figure 4.5 Stability study of the liposomes – Zeta Potential

Zeta potential (mV) and the standard deviation (mV) is given for every BSA/lipid molar ratio χ.
t_0 indicates the first time the zeta potential was read, which was immediately after the liposome preparation. The measurements read when the samples were one week old are indicated by t_1, two weeks old by t_2 and so on.

If the size distributions (Figure 4.4) of the BSA/lipid molar ratios (except for the 0.938 BSA/lipid molar ratio) are observed, it can be concluded that until the second or third week the formulations were stable. The smallest BSA/lipid molar ratio (0.752) has shown stability until the end of the studies. All the other formulations have greatly increased their sizes after week 2 or 3, indicating aggregation, and thus lack of stability.

For the lowest BSA/lipid ratios, the surface charge was initially positive, revealing that BSA was encapsulated inside the nanoparticle and not adsorbed at its surface. The highly positively charged liposomes (BSA/lipid ratio of 0.752) assured the stability of this formulation until the end of the project, since repulsion of the charged nanoparticles avoid aggregation. However, it can be observed in Figure 4.5 that the zeta-potential is becoming less positive in the BSA/lipid ratio of 0.752 and became negative in BSA/lipid ratio of 0.883. It is possible that BSA is being slowly dislocated from the interior of the vesicle to its surface. The later formulation (0.883) reached a negative value similar to the formulations with

higher BSA/lipid ratio, but the surface charge was not enough to guarantee repulsion between the liposomes and thus aggregation was observed from the third week (Figure 4.4).

From the BSA/lipid molar ratio of 0.938, there was a neutralization of the charge due to the electrostatic interaction between negatively charged BSA and positively charged liposomes. Because the surface charge of the nanoparticle was almost neutral already from the beginning, the BSA/lipid molar ratio of 0.938 formulation has always been highly unstable. There was not enough charge to guarantee repulsion between the liposomes which resulted in a quickly aggregation of the liposomes (Figure 4.4).

Regarding the highest molar fractions of BSA/lipid, their negative surface charge was attained by the BSA adsorbed to the liposome's surface and this negatively charged surface assured some stability during the first 3 weeks. However, Figure 4.5. shows that the zeta potential values of the highest molar fractions of BSA/lipid become less negative, indicating a possible release of BSA from the surface of the nanoparticle. This makes the surface of the liposomes less charged and thus more prone to aggregate as observed by the big size increase obtained from the fourth week.

4.1.3. DODAB:MO (1:2) liposomes prepared with overnight aging

Besides preparing liposomes by the normal method, an overnight aging procedure was tested to study the effect on the stability of this particular liposomal formulation. As it can be seen in Table 4.1, both the standard deviation associated to the size measurements and the PDI were quite high due to the fact that many aggregates are found. Trying to solve that problem, the liposome suspension is filtered using a non-pyrogenic sterile-R-filter is supplied by Sarstedt (Nümbrecht, Germany) of 0.45µm. The results are shown in Figure 4.3. Normally, big aggregates do not pass the filter and this probably did not happen. However, because of the stress that was exerted on the liposomes, they became unstable and formed again big aggregates immediately after filtering.

Table 4.1 Particle size (d.nm), St. Dev. (d.nm) and PDI of each BSA/lipid molar ratio of the liposomes prepared with an overnight aging procedure.

BSA/lipid mole fraction χ	0.752	0.883	0.938	0.968	0.987
Particle size (d.nm)	252.43	144.0	1575.33	357.9	147.10
St.Dev. (d.nm)	151.90	118.85	153.73	196.11	96.28
PDI	0.297	0.460	0.593	0.604	0.353

Table 4.2 Particle size (d.nm), standard deviation (d.nm) and PDI of each BSA/lipid molar ratio after filtration of the liposomes prepared with an overnight aging procedure.

BSA/lipid mole fraction χ	0.752	0.883	0.938	0.968	0.987
Particle size (d.nm)	402.1	100.7	314.9	68.7	40.4
St.Dev. (d.nm)	28.0	1.6	323.8	2.8	2.4
PDI	0.610	0.591	0.521	0.970	1.000

Both the standard deviation associated to the size measurements and the PDI of the filtrated liposomes were rather high. This is due to the fact that all samples but the liposomes with a molar ratio of 0.883 showed a small percentage of big aggregates. Also free BSA (small particle size peaks) and a small amount of normal liposomes are found in each sample. It suggests that after the filtering the stressed particles aggregated again.

4.1.4. DODAB:MO (1:2) liposomes prepared with different extrusion cycles

In order to optimize the BSA/liposomes preparation procedure different extrusion cycles were also tested for two BSA/lipid molar fractions (the ones that presented the highest PDI) and the results of the nanoparticle size is presented on Table 4.3 and Table 4.4.

Table 4.3 Mean particle size (d.nm) and standard deviation (d.nm) of the different peaks that were found and measured in the samples with a BSA/lipid mole ratio of 0.987.

5x400nm			5x400nm + 5x200nm		
PDI = 0.521			PDI = 0.502		
	Size (d.nm)	St.Dev (d.nm)		Size (d.nm)	St.Dev (d.nm)
Peak 1	7	4	Peak 1	7	3
Peak 2	167	12	Peak 2	175	215
Almost no aggregates were found.			Peak 3	4629	1422

Table 4.4 Mean particle size (d.nm) and standard deviation (d.nm) of the different peaks that were found and measured in the samples with a BSA/lipid mole ratio of 0.968.

5x400nm			5x400nm + 5x200nm		
PDI = 0.643			PDI = 0.502		
	Size (d.nm)	St.Dev (d.nm)		Size (d.nm)	St.Dev (d.nm)
Peak 1	9	4	Peak 1	8	3
Peak 2	117	57	Peak 2	160	109
Peak 3	1611	1421	Peak 3	1999	150

All samples present a high PDI value which is in agreement with the fact of the intensity distributions having more than one peak. This indicates that particles with different

sizes are found. The smallest sizes distribution (Peak 1 in Table 4.3 and Table 4.4) can be attributed to BSA which is not encapsulated. The bigger particle sizes belong to liposomes or BSA aggregates. The sizes of the liposomes encapsulated with BSA that were extruded by a 400 nm polycarbonate filter (5x400nm) are smaller and present a lower standard deviation than the ones which were further extruded through a smaller pore sized membrane (5x400nm+5x200nm).

From the results obtained, it seems that an extensive extrusion or an extrusion through narrow pore filters has no beneficial effect in terms of size optimization of the resultant nanoparticles. The particle size is not reduced and the distribution is still not monodisperse. It is even more unstable to extrude them through a narrower pore size, because of the stress that is put on the liposomes. Forcing the particles disposes the protein in such a way that it will aggregate easily.

4.2. DETERMINATION OF BSA ENCAPSULATION EFFICIENCY

4.2.1. Quantification of BSA via UV-VIS spectroscopy

To quantify BSA in liposomes and determine BSA encapsulation efficiency it is first necessary to obtain a direct correlation between BSA absorbance and BSA concentration. This was achieved by determining BSA molar absortivity by the measurement of UV-VIS absorbance of BSA standards in water (Figure 4.6).

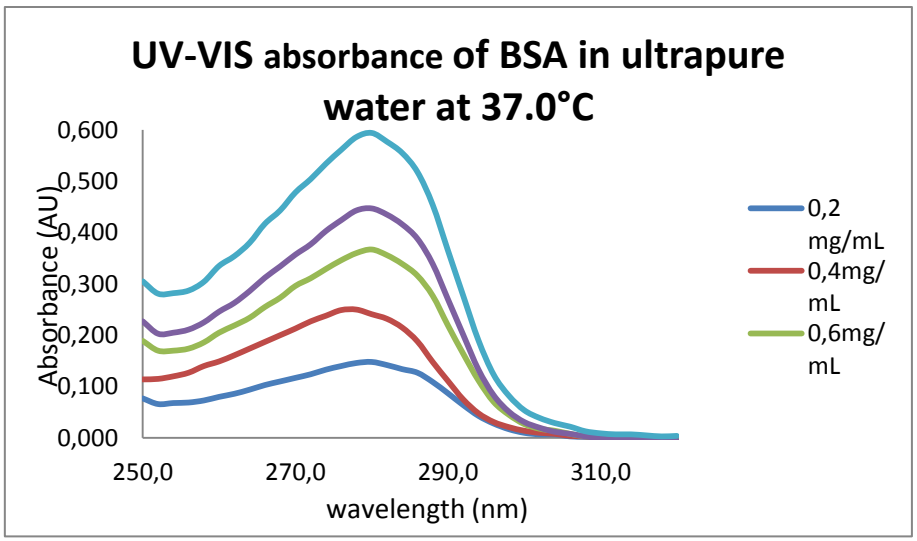

Figure 4.6 UV-visible absorbance spectrum from 250.0nm to 500.0nm of BSA in ultrapure water measured at a temperature of 37.0°C. BSA standard concentrations vary between 0.2mg/mL and 1.0mg/mL.

The maximal UV-visible absorbance of BSA in ultrapure water at a temperature of 37.0°C is found at 280.0nm. Consequently, the calibration curve is plot, displaying the absorbance of each standard at a wavelength of 280.0nm and is shown in Figure 4.7

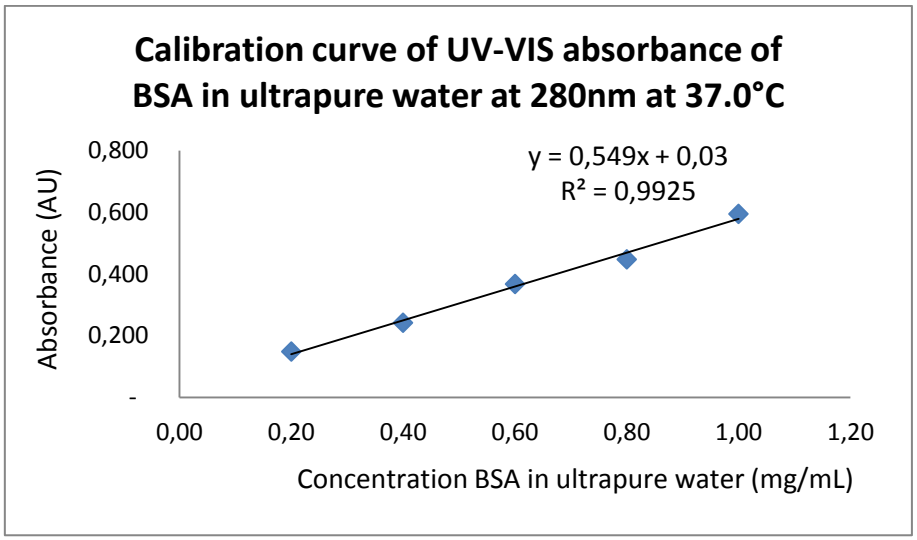

Figure 4.7 Calibration curve the UV-visible absorbance of BSA standards in ultrapure water at the maximum wavelength of absorption of 280nm, measured at a temperature of 37°C.

4.2.2. Quantification of BSA via fluorescence

4.2.2.1. Determination of BSA intrinsic fluorescence

Before fluorescence was used to determine the BSA concentration, it had to be proven that BSA emits light upon excitation. This can be done by means of reading the emission of a sample at three different excitation wavelengths as shown in Figure 4.8

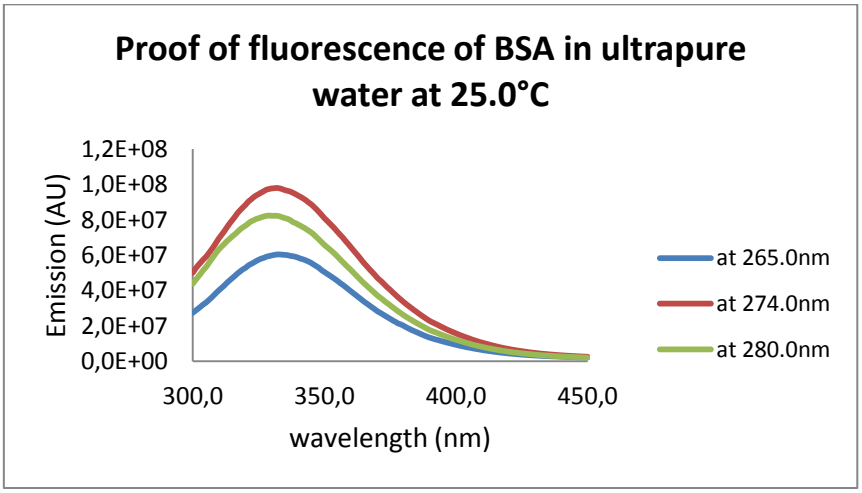

Figure 4.8 Intensity of emission of BSA in ultrapure water at a temperature of 25°C at different excitation wavelengths (265.0, 274.0, 280.0nm).

Because there is no significant deviation in maximum wavelength of the peaks to be seen in the graph, it can be concluded that the peaks truly originate from the intrinsic fluorescent properties of BSA in ultrapure water. The intensity of emission has its maximum

when a λ_{ex} of 274.0nm is used. When the emission is measured at different excitation wavelengths (such as 265.0 and 280.0nm), the intensity is lower.

The encapsulation efficiency assay was carried out several times. Only the encapsulation efficiency test results of one batch of samples is included in this paper. The other batches were excluded because they were either prepared using a different method (overnight aging) or the assay was carried out when the samples were much older and lost their stability.

After the separation and dilution, the fluorescence of the pellet and supernatant was read. The emission spectra of the pellet and the supernatant are shown respectively in Figure 4.9 and Figure 4.10. As there is scattering of the light due to the lipid particles the first derivative of the emission spectra is calculated (Figure 4.11 and Figure 4.12). Also the first derivative of the BSA emission spectra needs to be calculated (Figure 4.13 and Figure 4.14), because the data from the first derivative of the pellet and the supernatant will be used to calculate the encapsulation efficiency. Two calibration curves are drawn, each one with the data of emission found at the maxima of the first derivative of the pellet and supernatant (333nm and 380nm).

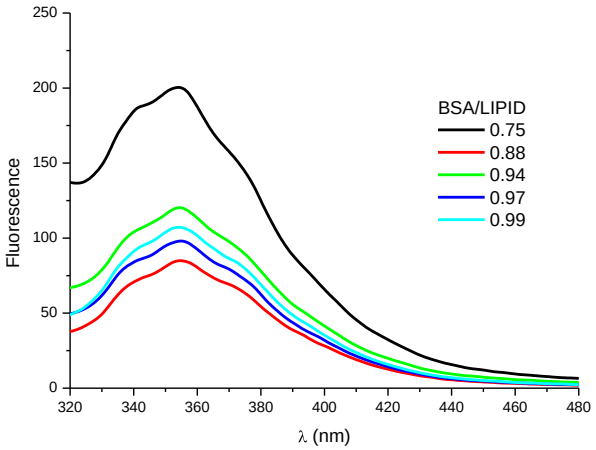

Figure 4.9 Emission spectra of the pellets of each BSA/lipid ratio after centrifugation

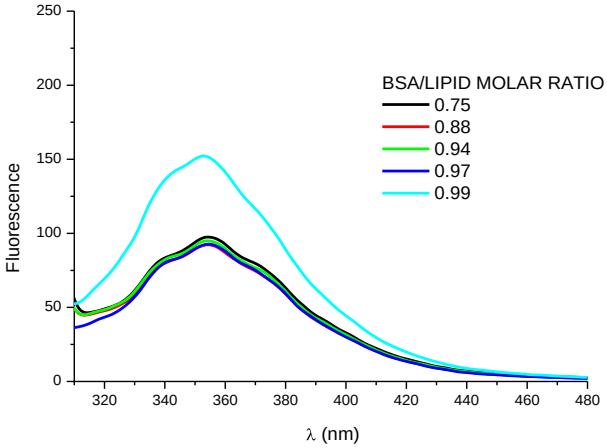

Figure 4.10 Emission spectra of the supernatants of each BSA/lipid ratio after centrifugation

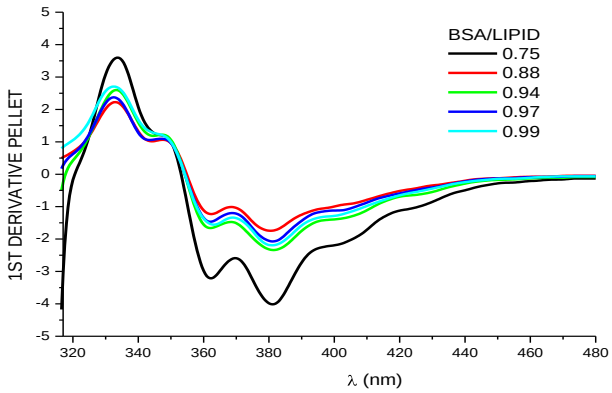

Figure 4.11 First derivative of the emission spectra of the pellets for each BSA/lipid ratio after centrifugation

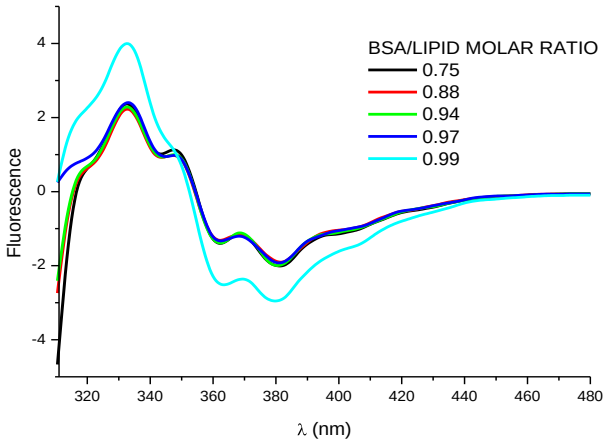

Figure 4.12 First derivative of the emission spectra of the supernatants for each BSA/lipid ratio after centrifugation

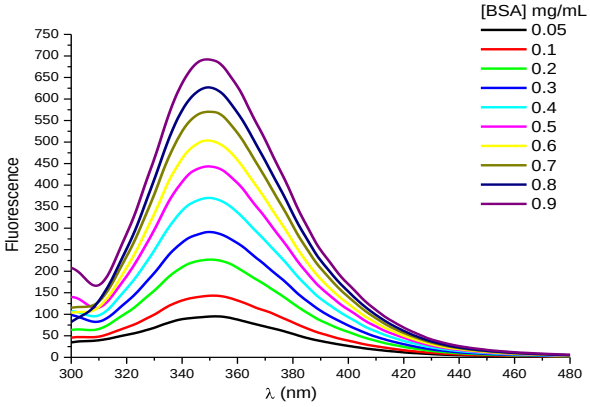

Figure 4.13 Emission spectra of BSA in ultrapure water at λ_{exc} of 292.0nm and 25.0°C

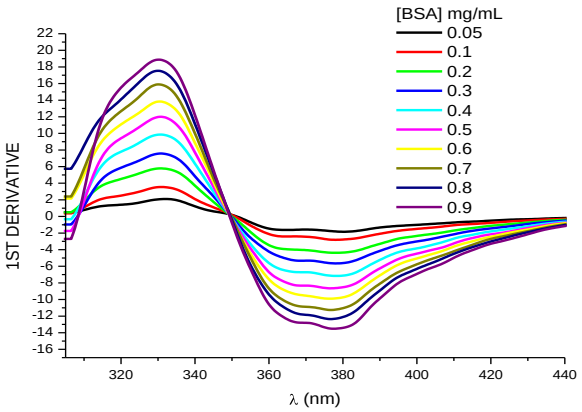

Figure 4.14 First derivative of the emission spectra of BSA in ultrapure water

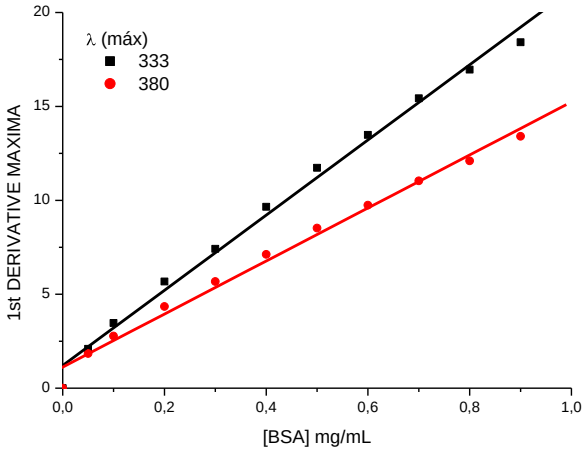

Figure 4.15 Calibration curves of BSA in ultrapure water at two different wavelengths

LINEAR FIT EQUATIONS Y=AX+B

	λ=333 nm	λ=380 nm
A	21.9	15.9
B	0.0	0.0
R	0.995	0.998

DERIVATIVES

λ 333nm is the 1ST maximum of supernatant and pellet

λ 380nm is the 2ND maximum of supernatant and pellet

λ 331nm and 378nm are the maximum of standards

Table 4.5 Data encapsulation efficiency assay(%)

BSA/LIPID mole ratio χ	Absorbance pellet (AU)		$f_{dilution}$	Concentration pellet (mg/mL)		Absorbance supernatant (AU)		$f_{dilution}$	Concentration supernatant (mg/mL)	
	λ=333nm	λ=380nm		λ=333nm	λ=380nm	λ=333 nm	λ=380nm		λ=333 nm	λ=380nm
0.725	3.6	4.0	0.097	1.68	2.58	2.4	2.0	0.913	0.12	0.14
0.938	2.6	2.3	0.098	1.21	1.49	2.3	2.0	0.912	0.11	0.14
0.968	2.4	2.1	0.098	1.10	1.32	2.4	1.9	0.887	0.12	0.14
0.987	2.7	2.2	0.093	1.32	1.48	4.0	3.0	0.929	0.20	0.20

BSA/lipid mole ratio χ	ENCAPSULATION (%)		ENCAPSULATION (%)	
	λ=333nm	λ=380nm	AVERAGE	St.Dev.
0.725	93.45	94.95	94.20	1.06
0.938	91.38	91.54	91.46	0.12
0.968	89.91	90.67	90.29	0.54
0.987	87.1	88.08	87.59	0.69

4.3. CIRCULAR DICHROISM

CD is an excellent method of determining the secondary structure of proteins. When the chromophores of the amides of the polypeptide backbone of proteins are aligned in arrays, their optical transitions are shifted or split into multiple transitions as a result of 'exciton' interactions (66). The result is that different structural elements have characteristic CD spectra (Figure 3.1). For example, α-helical proteins have negative bands at 222nm and 208nm and a positive band at 193nm (67). Proteins with well-defined antiparallel β-pleated sheets (β-helices) have negative bands at 218nm and positive bands at 195nm (67), whereas disordered proteins have very low ellipticity above 210nm and negative bands near 195nm (67).

The near-UV CD for all the BSA/lipid molar ratios were measured, but it was only possible to obtain reliable plots for the last two BSA/lipid molar ratios. This was due to the high light scattering produced by the increase of lipid concentration that greatly diminishes the signal to noise ratio. As it is possible to see in Figure 4.16, for higher lipid concentrations the dynode voltage goes above 500 volts. At these values the data are often described as very noisy and unreliable (67).

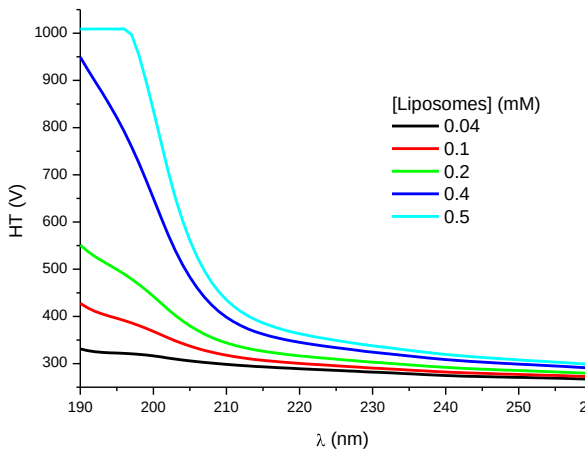

Figure 4.16 High tension voltage (V) plots obtained for increasing concentration of liposomes

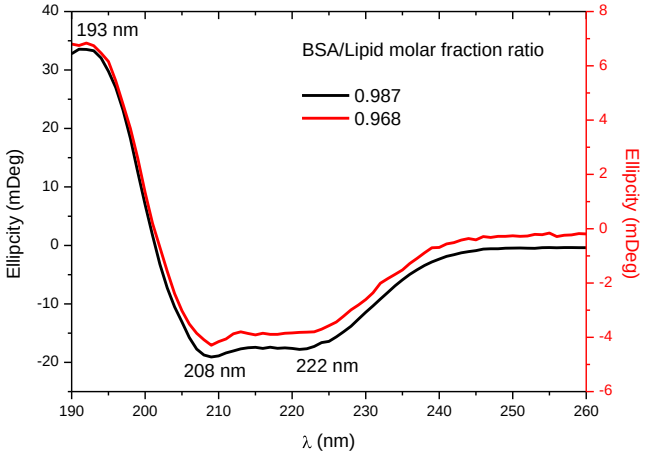

Figure 4.17 High tension voltage (V) plots obtained for increasing concentration of liposomes

Our interest in measuring CD-spectra of the BSA/liposome nanoparticles was based on the reported studies that indicate that the presence of lipids may disrupt the native α-helical structure of BSA, which might have consequences in local unfolding and a partial opening of hydrophobic pockets between domains, 34,42 leading to higher content of β-sheet structures (68). However, the near-UV CD of BSA/lipid ratios of 0.987 and 0.968 demonstrated that there had been no alteration of BSA secondary structure upon adsorption of the protein to the lipids. Indeed, the CD spectra is typical of BSA α-helical normal secondary structure presenting negative bands at 222nm and 208nm and a positive band at 193nm (Figure 4.17).

4.4. DETERMINATION OF BSA PARTITION COEFFICIENT

Intrinsic tryptophan and tyrosine fluorescence (λ_{exc} = 274nm) was utilized to assess the binding of liposomes to BSA. Structural rearrangements may result in the residue being more or less exposed to solvent and a resultant shift in the wavelength of maximal fluorescence emission ($\lambda_{em,max}$) or a reduction in the quantum yield (fluorescence intensity) of the residue due to quenching by newly adjacent residues (78).

The addition of increasing concentrations of liposomes (from 0 to 0.752 BSA/lipid molar fractions) has caused a shift of 4nm of the λ_{max} (from 350nm to 354nm) of BSA indicating that the protein is incorporated in the hydrophobic part of the lipid bilayer (Figure 4.18). This shift is consistent with zeta-potential results that indicate that for lower BSA/lipid

molar fractions BSA must be encapsulated inside of the liposomes. The addition of DODAB:MO (1:2) liposomes also decreased the intrinsic fluorescence intensity of BSA (approximately 36%) (Figure 4.18). A similar fluorescence quenching (of approximately 40%) has been observed as a result of the interaction of several albumin types with liposomes of DPPC (68).

The derivative spectra of the lipids in the absence of BSA present spectral bands that interfere with the spectral bands of BSA. Therefore, it is necessary to find the best wavelength were the signal of the lipids is reduced to calculate the partition coefficient by band analysis of BSA samples. In Figure 4.19 the chosen wavelength is 324.5nm. The K_p values were obtained by fitting Equation (3.5) to experimental first-derivative spectrofluorimetry data (Dt vs. [L]) for a fixed BSA concentration (0.1 mg/mL), using a nonlinear least squares regression method (65) at the wavelength where the scattering is eliminated (Figure 4.20).

The same procedure was made in the second derivative of the emission spectra (Figure 4.21). The best wavelength, where the signal of the lipids is reduced, was also chosen to calculate the partition coefficient by band analysis of BSA samples.

Lipophilicity means the tendency of the compound to partition between lipophilic phase (in this case DODAB:MO (1:2) liposomes) and polar aqueous phase, and the value of lipophilicity most commonly refers to the logarithm of the partition coefficient P (logP) between these two phases. The K_p of BSA between the lipid phase (DODAB:MO (1:2) liposomes) and the aqueous phase was determined as LogP = 5,38 ± 0,18 indicating a high lipophilicity of the protein and high distribution of this protein in the lipid media.

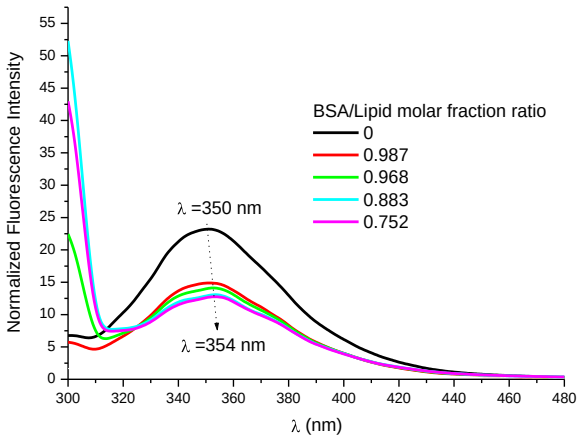

Figure 4.18 Representative intrinsic fluorescence emission spectra (λ_{exc} = 274nm) of at least three separate experiments for five BSA samples in the absence (black line) and presence (coloured lines) of DODAB:MO (2:1) liposomes (at different BSA/lipid mole ratios in water at 25 °C)

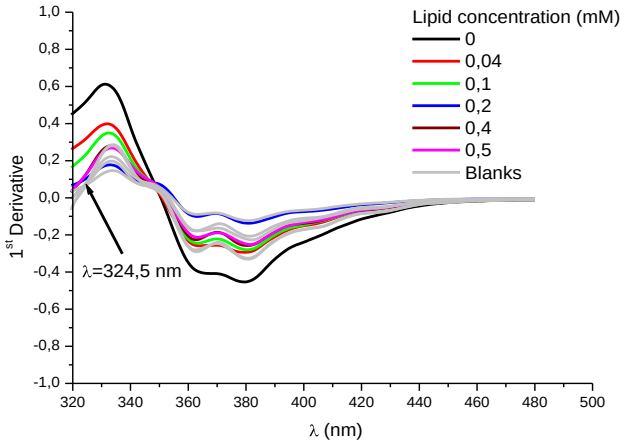

Figure 4.19 First derivative of the emission spectra of BSA with increasing amount of lipid (colored spectra) and the correspondent first derivative spectra of lipid references, containing the same amount of lipid and no BSA (grey lines)

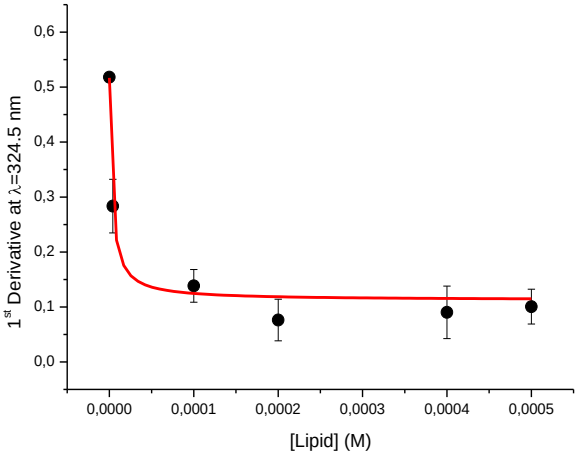

Figure 4.20 The curve represents the best fit by Eq. (3.5) to experimental first-derivative spectrophotometric data (Dt vs. [L]) using a nonlinear least squares regression method at wavelength 324.5nm where the scattering is eliminated.

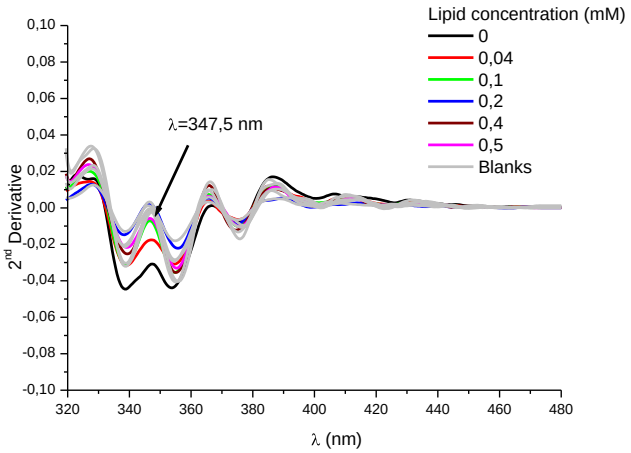

Figure 4.21 Second derivative of the emission spectra of BSA with increasing amount of lipid (colored spectra) and the correspondent first derivative spectra of lipid references, containing the same amount of lipid and no BSA (grey lines).

4.5. CONTROLLED RELEASE ASSAY

4.5.1. BSA in acetate buffer (pH 5.0)

4.5.1.1. UV-visible spectroscopy

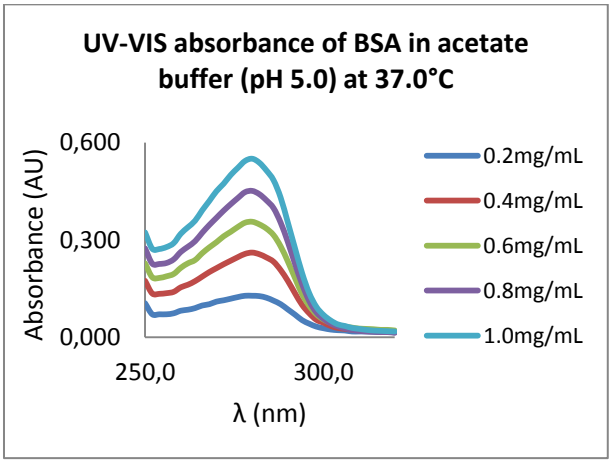

Figure 4.22 UV-visible absorbance spectrum of BSA in acetate buffer (pH 5.0). Sample temperature was set on 37.0°C.

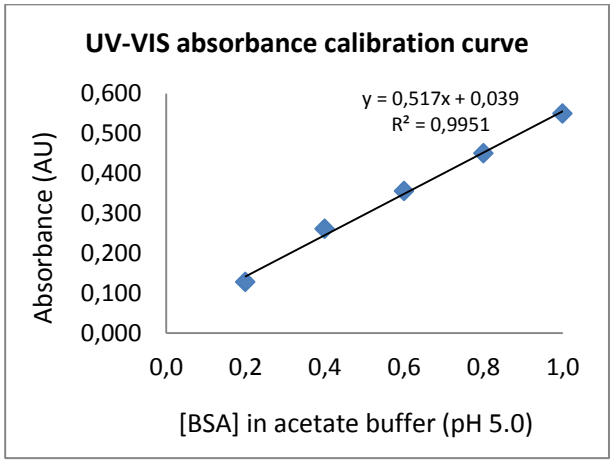

Figure 4.23 Calibration curve of UV-visible absorbance of BSA in acetate buffer (pH 5.0), read at the wavelength of maximum intensity of 280.0nm and a temperature of 37.0°C.

The maximum UV-visible absorbance of BSA in acetate buffer (pH 5.0) at a temperature of 37.0°C is found at 280.0nm. The calibration curve is drawn using the absorbance values measured at a wavelength of 280.0nm

4.5.1.2. Fluorescence

<u>Proof of fluorescence</u>

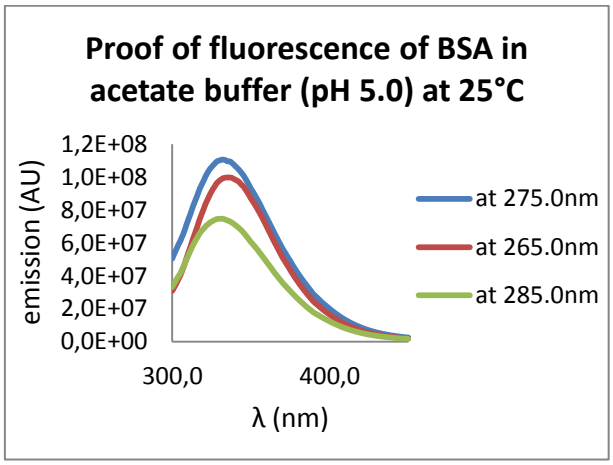

Figure 4.24 Intensity of emission of BSA in acetate buffer (pH 5.0). Samples were read at a temperature of 25°C at different excitation wavelengths (265.0nm, 275.0nm, 285.0nm).

The curves measured at an excitation wavelength of 265.0 and 285.0nm are not too much deviated in the maximum wavelength in comparison with the one measured at 275.0nm. It can be stated that the fluorescence emission peaks truly originate from the fluorescent properties of BSA in an acetate buffer with pH 5.0. The intensity of emission has its maximum at 275.0nm.

Emission

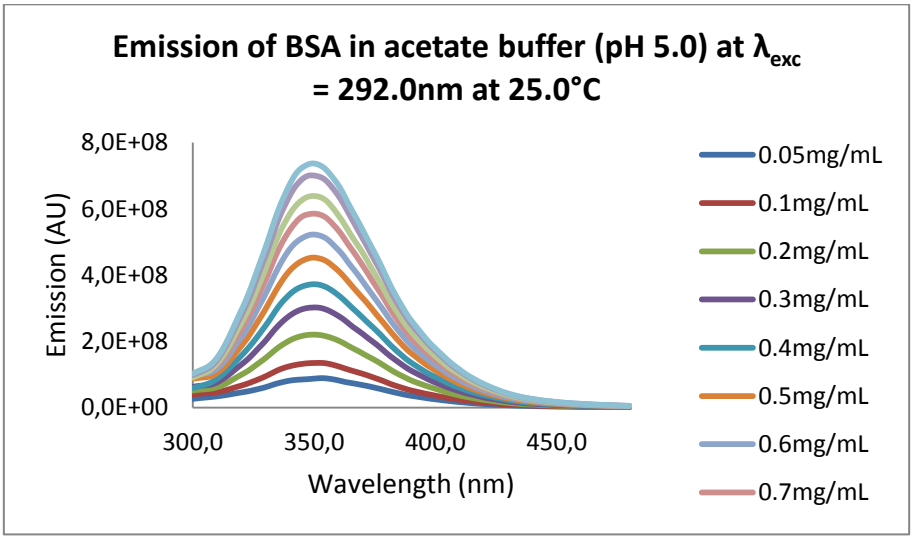

Figure 4.25 Emission spectrum of BSA in acetate buffer (pH 5.0) at 25.0°C. BSA is excited at 292.0nm

At a temperature of 25.0°C, an excitation wavelength of 292.0nm and in a acetate buffer solution which has a pH 5.0, BSA has a maximal fluorescence emission of 349.5nm.

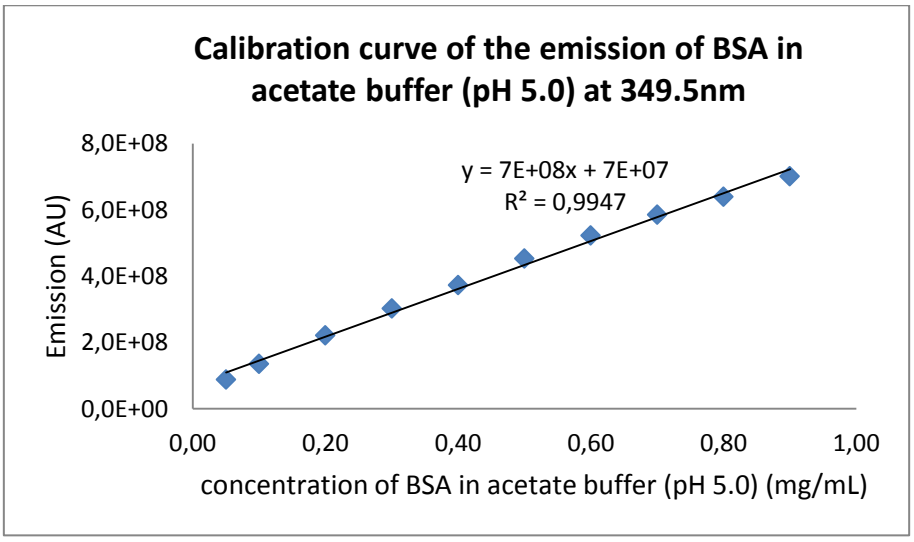

Figure 4.26 Calibration curve of the emission of BSA in acetate buffer (pH 5.0) at the wavelength of maximum emission (349.5nm). BSA is excited at 292.0nm and read at a temperature of 25.0°C.

4.5.2. BSA in HEPES buffer (pH 7.4)

4.5.2.1. UV-visible spectroscopy

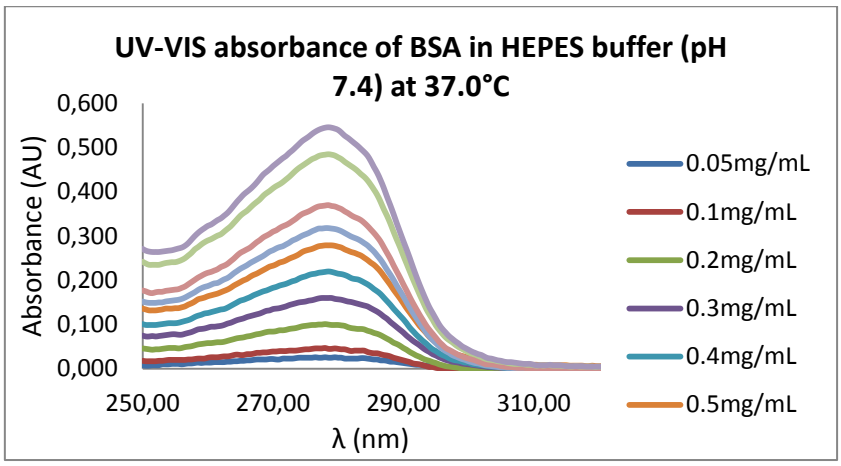

Figure 4.27 UV-visible absorbance spectrum of BSA in HEPES buffer (pH 7.4) at a temperature of 37.0°C.

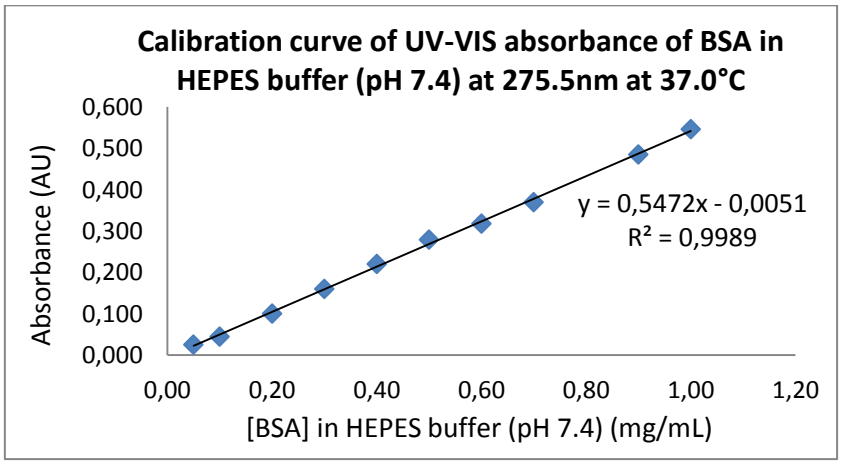

Figure 4.28 Calibration curve of UV-VIS absorbance of BSA in HEPES buffer (pH 7.4), read at the wavelength of maximum absorbance (275.5nm) at a temperature of 37.0°C.

4.5.2.2. Fluorescence

Proof of fluorescence

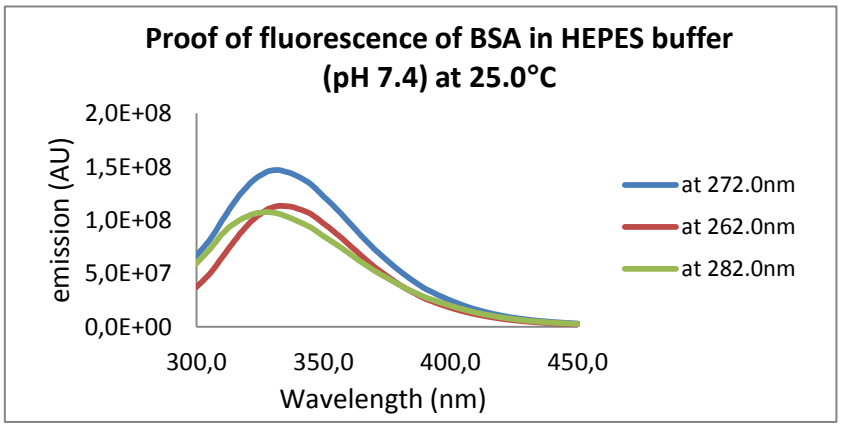

Figure 4.29 Intensity of the emission of BSA in HEPES buffer (pH 7.4). Samples were read at a temperature of 25.0°C at different excitation wavelengths (262.0nm, 272.0nm, 282.0nm).

The difference of the maximum wavelength of the curves measured at an excitation wavelength of 262.0 and 282.0nm is not too big in comparison with the one measured at 275.0nm. It can be stated that the fluorescence emission peaks truly originate from the fluorescent properties of BSA in a HEPES buffer with pH 5.0. The intensity of emission has its maximum at 275.0nm.

Emission

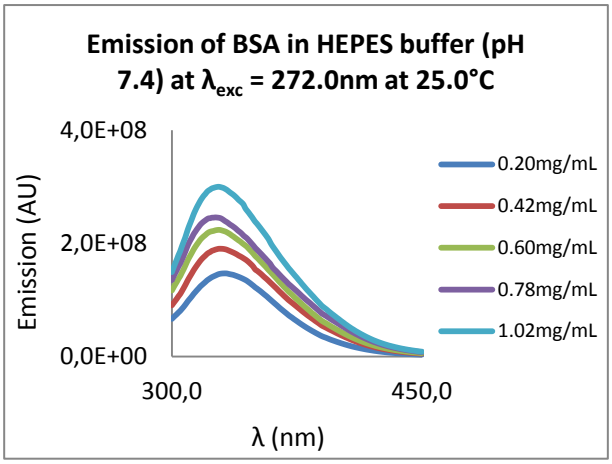

Figure 4.30 Emission spectrum of BSA in HEPES buffer (pH 7.4), read at 25.0°C. BSA is excited at 272.0nm

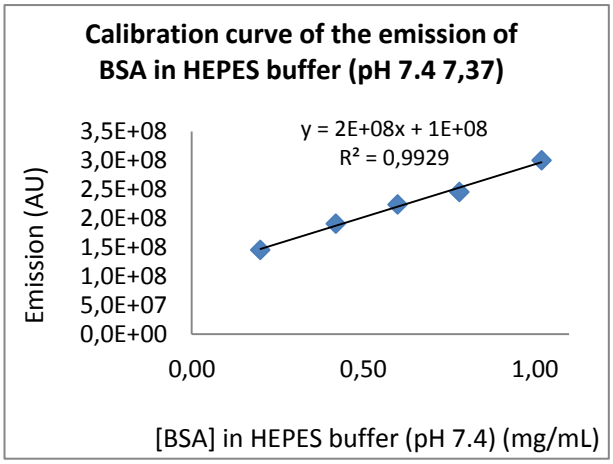

Figure 4.31 Calibration curve of the emission of BSA in HEPES buffer (pH 7.4) at the wavelength of maximum intensity (328.0nm), read at a sample temperature of 25.0°C. BSA is excited at 272.0nm.

The fluorescence emission of BSA in a HEPES solution has a maximum at a wavelength of 328.0nm. The measurement are read at a temperature of 25°C and at an excitation wavelength of 272.0nm. The emission values at the wavelength of 328.0nm are used to draw the calibration curve.

5. DISCUSSION

5.1. LIPOSOMAL SIZE AND SURFACE CHARGE

Smaller liposomes are better for intravenous drug delivery and for reaching longer circulation times. In agreement to this in the current work the main goal was to produce liposomal nanoparticles containing BSA with sizes controlled preferably equal or less than 200nm. The liposomes production method was conditioned by several factors. Firstly, we could not use sonication procedures, which would produce small unilamellar vesicles (SUV) with lower sizes. The sonication energy of the probe would have causes BSA denaturation.

Therefore to reach an acceptable size of liposomes we have decided to perform the hydration method followed by extrusion, known as a good method to obtain large unilamellar vesicles (LUV) of controlled sizes, with homogeneous distribution of the size population. We have reached to the conclusion that increasing the number of extrusion steps, or using filters with smaller pores (e.g. 200nm and 100nm) originated more polydisperse liposomal formulations with a tendency to form big aggregates. A possible explanation for this is the fact that forcing BSA to pass through the pores might have caused some stress on the protein forcing it to change conformation and aggregate. Hence the most effective procedure to produce the liposomes was the hydration method to produce multilamellar vesicles (MLV) followed by extrusion by a relatively large pore filter (5 times through 400nm). This procedure produces liposomes with acceptable sizes and polidispersity (about 200nm and PDI 0.2 at least for formulations with smaller BSA/lipid ratios). The PDI values are higher than 0.1 and indicate that the formulation is not completely monodisperse. This is due to the presence of high MO content. Indeed, increasing MO content in the formulation has the advantage of originating a liposomal formulation with a mixture of lipid phases: DODAB forms a lamellar phase that encloses MO inverted non-lamellar phases (78).

The advantage of these enriched nanoparticles is the possibility of greatly increasing the encapsulation of lipophilic compounds, and in this case BSA inside the liposome. However, the presence of a phase mixture will obviously induce the formation of some heterogeneity in the liposomes dispersion. Further addition of BSA also causes an increase in

PDI because it can be bound to the surface of the vesicle, which leads to different particle sizes.

Also because of the high content of MO in the formulation, the process of aging (incubation of liposomes overnight at a temperature superior to the main transition temperature is favourable to condition the phases of the liposomes). In this particular liposome, monoolein is present. It is known that an increase in temperature has the same consequence as an increase in MO concentration, namely the formation of aggregates (10). MO changes the organisation and shape of the lipid vesicle and when the amount of MO (or in this case the temperature) is increased it can lead to unfavourable particle sizes and PDI values. The temperature alters many other different properties, such as the conformation of proteins. The effect of the temperature on the encapsulation cannot be predicted, because it is not known in which conformation BSA enters or absorbs onto the liposomes in a better or worse way. Knowing that the adsorption of BSA onto the particles influences the particle size, it can be stated that the particle size cannot be predicted for different temperatures. Also the fluidity of the vesicle is controlled by the temperature. When the solution is warmed up above the transition temperature, it is possible that the vesicle is fluid enough to capture and release BSA several times.

The surface charge of the nanoparticle is also essential regarding their shelf stability and efficiency to cross cell membranes. Neutral charged particles will be less stable and will aggregate as there is no repulsion between the surface charge of the NP in suspension. Charged vesicles on the other hand have higher shelf stability due to the repulsion between the nanoparticles that keeps them in a stable suspension. Positively charged liposomes have the further advantage of facilitating the cellular adhesion as cell membranes are slightly negatively charged. The surface charge of the BSA/DODAB:MO (1:2) liposomes was highly dependent of the BSA/lipid ratio. For low BSA/lipid ratios (e.g. 0.752 and 0.883) the liposomes were positively charged, indicating that BSA, which is negatively charged at the pH of the studies, was encapsulated inside of the particles. This positive surface charge is advantageous both in terms of shelf stability, providing repulsion between the liposomes, and in terms of membrane cell adhesion as the positive charges will have higher propensity to interact with slightly negatively charged cellular membranes. For higher BSA/lipid ratios

(e.g. 0.938, 0.968 and 0.987) the liposomes were negatively charged, indicating that BSA was adsorbed to the liposomal surface, neutralizing the positive charges from the DODAB ammonium group. In the case of BSA/lipid ratio of 0.938, the surface charge was only slightly negative and very close to neutrality. For BSA/lipid ratio above 0.938 BSA further covers the surface of the liposome with a negatively charge. The negative charge also confers some shelf stability, due to the repulsion between the negative vesicles. However as this negative charge is caused by the BSA adsorbed to the nanoparticle surface, the stability of the particles is dependent on the stability of the adsorbed protein. Figure 5.1 shows a prediction of the liposomal structure and BSA distribution in the liposomal NP.

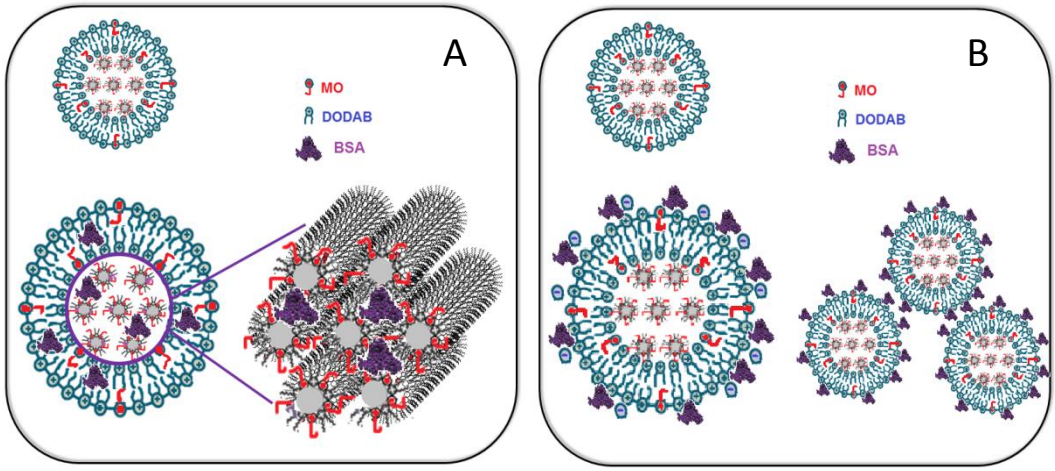

Figure 5.1 Schematic representation of the DODAB:MO (1:2) liposomes containing BSA. A – Represents the smallest BSA:liposomes molar ratios, where BSA is distributed inside the lamellar and non-lamellar inverted structures. B – Represents the highest BSA:liposomes molar ratios, where BSA is distributed adsorbed to the lamellar positive surface charge neutralizing this charge and promoting aggregation between de nanoparticles.

5.2. LIPOSOMAL STABILITY, ENCAPSULATION OF BSA AND PREDICTION OF ITS LOCATION IN THE LIPOSOMES

It has to be note down that the encapsulation assay was carried out 10 days after the liposome preparation. In this moment the liposomes particle size and zeta potential are between t_1 and t_2 (Figure 4.4 and Figure 4.5).

As is written in 4.1.2.3, the liposomes with a BSA/lipid mole ratio of 0.752 are more or less stable during 8 weeks. The ζ-potential was highly positive, nevertheless decreased in comparison with blank DODAB:MO (1:2) liposomes. This indicates that almost all BSA is incorporated inside the particles. As no free BSA was found by DLS measurements, it can be concluded that at the moment of the encapsulation assay many BSA molecules were

encapsulated inside the liposomes. However, there is a small amount of BSA attached to the surface. This is endorsed by the results of the encapsulation assay which shows an encapsulation efficiency of 94.20%. In these liposomes, there is less protein in comparison with the lipid fraction. The protein has more opportunity to get completely incorporated into the vesicles. The decrease in zeta potential in the next weeks is probably due to the slowly release of the encapsulated BSA. The negatively charged BSA will then electrostatically interact with the positively charged liposomes. Consequently, the charge of the liposomes will decrease.

Liposomes with a BSA/lipid mole ratio of 0.883 have a smaller particle size than the blank DODAB:MO (1:2) liposomes immediately after the preparation. It suggests that BSA is not attached to the surface of the particle, because this would have increased the size. Also the zeta potential is quite high and the DLS measurements showed no free BSA. It can be concluded that BSA is incorporated in the lipid particles promoting their condensation. The zeta potential decreases because of the same reason as mentioned above. It can be seen that after the decrease in zeta potential, the charge increases again a bit. This can be due to the fact that the negatively charged BSA covering the liposomes will interact with other positively charged DODAB:MO (1:2) particles which are less coated with BSA. This interaction screens the negative charge from the BSA on the surface partially and the zeta potential will increase. If such an interaction would occur, then the size would change too, because two or more particles will aggregate together. Indeed, the big particle size that is seen after week 2 can be traced back to first the release and interaction of BSA and the liposome and second the aggregation of two or more particles.

The zeta potential of the liposomes with a BSA/lipid mole ratio of 0.938 was negative from in the beginning. The encapsulation efficiency is 91.46%. The amount of protein is higher than in the previous samples. BSA is as much encapsulated as possible, but when the amount of protein increases, BSA will start to absorb on the surface too. If the information of both the encapsulation assay as the zeta potential is combined it can be stated that BSA is mainly on attached to the outside of the lipid particles. Also the measurements of the particle size endorse this theory. The size increases quickly, which corresponds with BSA that

is adsorbed on the liposomes. After week 3 the ζ-potential is around zero, which causes easily the aggregation of particles, which is also confirmed by the increase in particle size.

The liposomes with a BSA/lipid mole ratio of 0.968 showed a negative ζ-potential directly after the preparation. The older the samples, the more positive they were charged, until week 3. This situation is the opposite of what happened with the first two samples. Instead of a decrease, there is now an increase in zeta potential. At week 3, a part of the cationic lipid is still exposed to the outside environment, but most part is covered by BSA, because the potential is not as positive as that of blank liposomes. It is clear that initially BSA was absorbed onto the particle surface. In time the BSA cannot move to the inside. The negative BSA/lipid complex can attract cationic liposomes which cover the negative charge of BSA. If this happens, the charge of the entire complex will increase. The particle size will increase too, which is in fact the case. Afterwards, the potential is close to zero again, which causes an unstable situation and particles tend to form big aggregates. The encapsulation has an efficiency of 90.29%, which corresponds with the negative potential. BSA is indeed attached to the liposomes.

The highest protein concentration is found in the samples with a BSA/lipid mole ratio of 0.987. The zeta potential is negative. The modulus is not greater than 30mV, but it is still quite high and more or less the same over a period of 3 weeks. Also the particle size endorses this stability. However the PDI is quite high, which is probably due to the presence of the protein BSA. After 3 weeks the zeta potential increases and measures close to zero what causes again the instability of the particles, which is also seen in the results of the particle size.

Intrinsic fluorescence measurements and Kp determination corroborate the location of BSA in different parts of the liposome according to the BSA/lipid molar fractions.

5.3. BSA FUNCTIONALITY

BSA functionality depends on the maintenance of its typical secondary structure that assures that the protein displays the drug binding sites available. Upon BSA encapsulation in liposomes, its secondary structure is maintained in an α-helix conformation, which is a good sign to obtain a functional particle able to carry drugs.

6. CONCLUSION

The stability and encapsulation efficiency are different for each BSA/lipid mole ratio. The liposomes prepared with less protein (BSA/lipid mole ratio of 0.752) appeared to be the most stable protein/lipid ratio. This ratio had also the highest encapsulation efficiency (94.20%). The BSA/DODAB:MO (1:2) with a mole ratio of 0.752 showed great economical and therapeutical potential to be further analysed. Nevertheless, the BSA/lipid mole ratios of 0.968 and 0.987 also showed satisfying results with an encapsulation efficiency of 90.29% and 87.59% respectively.

Circular dichroism is measured it is important to determine how BSA reacts upon adsorption. Misfolded proteins can expose normally buried hydrophobic residues. This change could cause the particles to aggregate. The results showed that the secondary structure of BSA does not alterate upon adsorption of the protein to the lipids. The CD spectra is typical of BSA α-helical normal secondary structure presenting negative bands at 222nm and 208nm and a positive band at 193nm.

The partition coefficient of BSA between the lipid phase and the aqueous phase was determined as LogP = 5,38 ± 0,18. This gives proof of a high lipophilicity of the protein and high distribution of BSA in the lipid media.

All the results will be compared for the most promising BSA/lipid mole ratio, namely 0.752. BSA will be encapsulated with a high efficiency (94.20%), this means that BSA can either be adsorbed to the outside surface of the DODAB:MO (1:2) liposome or it can be incorporated into the vesicle. It can be concluded that BSA is incorporated into the vesicle if the zeta potential is considered. The partition coefficient gives more information about the exact location in the vesicle, it proves that BSA is lipophilic and prefers to be inside the lipid bilayer of the vesicle.

In the near future, the controlled release assay will be carried out. Because of the amphiphilic properties and pH dependent charge of BSA molecules, the liposomes should load and release drugs in a very efficient way in the human body. To study this release, pH

conditions of the gastrointestinal tract and blood circulation are simulated and the amount of released BSA at these pH values is quantified. This quantification will be used in *in vitro* controlled release assays on cell cultures which are planned to be carried out in continuation of the current work.

When in future, the formulations are tested on cell cultures and it turns out that the BSA/lipid ratio of 0.752 does not have a high efficiency, the *in vitro* effect of the two formulations with a higher BSA/lipid ratio can be explored too.

The particle size is slightly too big to ensure non-immunogenicity of the liposomes when administered intravenously. Other possible applications for these liposomes could be transdermal delivery of drugs. It is already proven *in vitro* that nanogels with BSA are able to penetrate the skin and deliver the hydrophilic proteins (25). This field of study can also be considered with the BSA/DODAB:MO (1:2) liposomes.

7. REFERENCES

7.1. BIBLIOGRAPHY

1. Togashi DM, Ryder AG, Mc Mahon D, Dunne P, McManus J. Fluorescence study of Bovine Serum Albumin and Ti and Sn oxide nanoparticles interactions - art. no. 66281K. P Soc Photo-Opt Ins. 2007;6628:K6281-K. PubMed PMID: WOS:000251475200041. English.
2. Kulkarni CV, Wachter W, Iglesias-Salto G, Engelskirchen S, Ahualli S. Monoolein: a magic lipid? Physical chemistry chemical physics : PCCP. 2011 Feb 28;13(8):3004-21. PubMed PMID: 21183976.
3. Escriba PV. Membrane-lipid therapy: a new approach in molecular medicine. Trends in molecular medicine. 2006 Jan;12(1):34-43. PubMed PMID: 16325472.
4. Chang WK, Tai YJ, Chiang CH, Hu CS, Hong PD, Yeh MK. The comparison of protein-entrapped liposomes and lipoparticles: preparation, characterization, and efficacy of cellular uptake. Int J Nanomed. 2011;6:2403-17. PubMed PMID: WOS:000297678800001. English.
5. Lamprecht A, Ubrich N, Hombreiro Perez M, Lehr C, Hoffman M, Maincent P. Biodegradable monodispersed nanoparticles prepared by pressure homogenization-emulsification. International journal of pharmaceutics. 1999 Jul 5;184(1):97-105. PubMed PMID: 10425355.
6. Ostro MJ, Cullis PR. Use of liposomes as injectable-drug delivery systems. American journal of hospital pharmacy. 1989 Aug;46(8):1576-87. PubMed PMID: 2672806.
7. Mokhtarieh AA, Davarpanah SJ, Lee MK. Ethanol treatment a Non-extrusion method for asymmetric liposome size optimization. Daru : journal of Faculty of Pharmacy, Tehran University of Medical Sciences. 2013;21(1):32. PubMed PMID: 23597170. Pubmed Central PMCID: PMC3637568.
8. Nogueira E, Loureiro A, Nogueira P, Freitas J, Almeida CR, Harmark J, et al. Liposome and protein based stealth nanoparticles. Faraday discussions. 2013;166:417-29. PubMed PMID: 24611291.
9. Jamroz D, Kepczynski M, Nowakowska M. Molecular structure of the dioctadecyldimethylammonium bromide (DODAB) bilayer. Langmuir : the ACS journal of surfaces and colloids. 2010 Oct 5;26(19):15076-9. PubMed PMID: 20804190.
10. Oliveira IM, Silva JP, Feitosa E, Marques EF, Castanheira EM, Real Oliveira ME. Aggregation behavior of aqueous dioctadecyldimethylammonium bromide/monoolein mixtures: a multitechnique investigation on the influence of composition and temperature. Journal of colloid and interface science. 2012 May 15;374(1):206-17. PubMed PMID: 22377488.
11. Mufamadi MS, Pillay V, Choonara YE, Du Toit LC, Modi G, Naidoo D, et al. A review on composite liposomal technologies for specialized drug delivery. Journal of drug delivery. 2011;2011:939851. PubMed PMID: 21490759. Pubmed Central PMCID: PMC3065812.
12. Ganem-Quintanar A, Quintanar-Guerrero D, Buri P. Monoolein: a review of the pharmaceutical applications. Drug development and industrial pharmacy. 2000 Aug;26(8):809-20. PubMed PMID: 10900537.
13. El Kadi N, Taulier N, Le Huerou JY, Gindre M, Urbach W, Nwigwe I, et al. Unfolding and refolding of bovine serum albumin at acid pH: ultrasound and structural studies. Biophysical journal. 2006 Nov 1;91(9):3397-404. PubMed PMID: 16861279. Pubmed Central PMCID: PMC1614494.
14. Zu Y, Meng L, Zhao X, Ge Y, Yu X, Zhang Y, et al. Preparation of 10-hydroxycamptothecin-loaded glycyrrhizic acid-conjugated bovine serum albumin nanoparticles for hepatocellular carcinoma-targeted drug delivery. Int J Nanomedicine. 2013;8:1207-22. PubMed PMID: 23569373. Pubmed Central PMCID: PMC3615927.
15. Jung SH, Kim SK, Jung SH, Kim EH, Cho SH, Jeong KS, et al. Increased stability in plasma and enhanced cellular uptake of thermally denatured albumin-coated liposomes. Colloids and surfaces B, Biointerfaces. 2010 Apr 1;76(2):434-40. PubMed PMID: 20036109.
16. Walker JM. The Protein Protocols Handbook. Dordrecht: Springer,; 2009.
17. Ju C, Mo R, Xue J, Zhang L, Zhao Z, Xue L, et al. Sequential Intra-Intercellular Nanoparticle Delivery System for Deep Tumor Penetration. Angewandte Chemie. 2014 Apr 16. PubMed PMID: 24740532.

18. Shen HJ, Shi H, Ma K, Xie M, Tang LL, Shen S, et al. Polyelectrolyte capsules packaging BSA gels for pH-controlled drug loading and release and their antitumor activity. Acta Biomater. 2013 Apr;9(4):6123-33. PubMed PMID: WOS:000316526700024. English.
19. Liu Y, Yao W, Wang S, Di G, Zheng Q, Chen A. Preparation and characterization of fucoidan-chitosan nanospheres by the sonification method. Journal of nanoscience and nanotechnology. 2014 May;14(5):3844-9. PubMed PMID: 24734649.
20. Jain S, Indulkar A, Harde H, Agrawal AK. Oral mucosal immunization using glucomannosylated bilosomes. Journal of biomedical nanotechnology. 2014 Jun;10(6):932-47. PubMed PMID: 24749389.
21. Mladenovska K, Kumbaradzi E, Dodov G, Makraduli L, Goracinova K. Biodegradation and drug release studies of BSA loaded gelatin microspheres. International journal of pharmaceutics. 2002 Aug 21;242(1-2):247-9. PubMed PMID: 12176256.
22. Chitkara D, Kumar N. BSA-PLGA-based core-shell nanoparticles as carrier system for water-soluble drugs. Pharmaceutical research. 2013 Sep;30(9):2396-409. PubMed PMID: 23756758.

23. Zheng Y, Song X, Darby M, Liang Y, He L, Cai Z, et al. Preparation and characterization of folate-poly(ethylene glycol)-grafted-trimethylchitosan for intracellular transport of protein through folate receptor-mediated endocytosis. Journal of biotechnology. 2010 Jan 1;145(1):47-53. PubMed PMID: 19770010.
24. Chang WK, Tai YJ, Chiang CH, Hu CS, Hong PD, Yeh MK. The comparison of protein-entrapped liposomes and lipoparticles: preparation, characterization, and efficacy of cellular uptake. Int J Nanomedicine. 2011;6:2403-17. PubMed PMID: 22072876. Pubmed Central PMCID: PMC3205135.
25. Choi WI, Lee JH, Kim JY, Kim JC, Kim YH, Tae G. Efficient skin permeation of soluble proteins via flexible and functional nano-carrier. Journal of controlled release : official journal of the Controlled Release Society. 2012 Jan 30;157(2):272-8. PubMed PMID: 21867735.
26. Zeng R, Tu M, Liu HW, Zhao JH, Zha ZG, Zhou CR. Preparation, structure and drug release behaviour of chitosan-based nanofibres. IET nanobiotechnology / IET. 2009 Mar;3(1):8-13. PubMed PMID: 19222301.
27. Jain S, Sharma RK, Vyas SP. Chitosan nanoparticles encapsulated vesicular systems for oral immunization: preparation, in-vitro and in-vivo characterization. The Journal of pharmacy and pharmacology. 2006 Mar;58(3):303-10. PubMed PMID: 16536896.
28. Guo R, Chen LL, Cai SS, Liu ZH, Zhu Y, Xue W, et al. Novel alginate coated hydrophobically modified chitosan polyelectrolyte complex for the delivery of BSA. J Mater Sci-Mater M. 2013 Sep;24(9):2093-100. PubMed PMID: WOS:000323289600002. English.
29. Su Z, Xing L, Chen Y, Xu Y, Yang F, Zhang C, et al. Lactoferrin Modified Poly (ethylene glycol)-Grafted BSA Nanoparticles as A Dual-Targeting Carrier for Treating Brain Gliomas. Molecular pharmaceutics. 2014 Apr 29. PubMed PMID: 24779677.
30. Zu Y, Zhang Y, Zhao X, Zhang Q, Liu Y, Jiang R. Optimization of the preparation process of vinblastine sulfate (VBLS)-loaded folate-conjugated bovine serum albumin (BSA) nanoparticles for tumor-targeted drug delivery using response surface methodology (RSM). Int J Nanomedicine. 2009;4:321-33. PubMed PMID: 20054435. Pubmed Central PMCID: PMC2802044.
31. Liu Z, Dong C, Wang X, Wang H, Li W, Tan J, et al. Self-assembled biodegradable protein-polymer vesicle as a tumor-targeted nanocarrier. ACS applied materials & interfaces. 2014 Feb 26;6(4):2393-400. PubMed PMID: 24456410.
32. Liu TY, Chen SY, Liu DM, Liou SC. On the study of BSA-loaded calcium-deficient hydroxyapatite nano-carriers for controlled drug delivery. Journal of controlled release : official journal of the Controlled Release Society. 2005 Sep 20;107(1):112-21. PubMed PMID: 15982777.
33. Liang X, Sun Y, Liu L, Ma X, Hu X, Fan J, et al. Folate-functionalized nanoparticles for controlled ergosta-4,6,8(14),22-tetraen-3-one delivery. International journal of pharmaceutics. 2013 Jan 30;441(1-2):1-8. PubMed PMID: 23262423.
34. Samanta B, Yan H, Fischer NO, Shi J, Jerry DJ, Rotello VM. Protein-passivated Fe(3)O(4) nanoparticles: low toxicity and rapid heating for thermal therapy. Journal of materials chemistry. 2008;18(11):1204-8. PubMed PMID: 19122852. Pubmed Central PMCID: PMC2593465.
35. Zhang B, Deng L, Xing J, Yang J, Dong A. Ternary complexes of poly(vinyl pyrrolidone)-graft-poly(2-dimethylaminoethyl methacrylate), DNA and bovine serum albumin for gene delivery. Journal of biomaterials science Polymer edition. 2013;24(1):45-60. PubMed PMID: 22289623.
36. Dakwar GR, Abu Hammad I, Popov M, Linder C, Grinberg S, Heldman E, et al. Delivery of proteins to the brain by bolaamphiphilic nano-sized vesicles. Journal of controlled release : official journal of the Controlled Release Society. 2012 Jun 10;160(2):315-21. PubMed PMID: 22261280.
37. Rejinold NS, Chennazhi KP, Tamura H, Nair SV, Rangasamy J. Multifunctional chitin nanogels for simultaneous drug delivery, bioimaging, and biosensing. ACS applied materials & interfaces. 2011 Sep;3(9):3654-65. PubMed PMID: 21863797.
38. Guo W, Li D, Zhu JA, Wei X, Men W, Yin D, et al. A magnetic nanoparticle stabilized gas containing emulsion for multimodal imaging and triggered drug release. Pharmaceutical research. 2014 Jun;31(6):1477-84. PubMed PMID: 24718918.
39. Huang D, Wang L, Dong Y, Pan X, Li G, Wu C. A novel technology using transscleral ultrasound to deliver protein loaded nanoparticles. European journal of pharmaceutics and biopharmaceutics : official journal of Arbeitsgemeinschaft fur Pharmazeutische Verfahrenstechnik eV. 2014 May 14. PubMed PMID: 24833007.
40. De Rosa E, Chiappini C, Fan D, Liu X, Ferrari M, Tasciotti E. Agarose surface coating influences intracellular accumulation and enhances payload stability of a nano-delivery system. Pharmaceutical research. 2011 Jul;28(7):1520-30. PubMed PMID: 21607779.
41. Yang SY, Yang JA, Kim ES, Jeon G, Oh EJ, Choi KY, et al. Single-file diffusion of protein drugs through cylindrical nanochannels. ACS nano. 2010 Jul 27;4(7):3817-22. PubMed PMID: 20507175.
42. Crisante F, Francolini I, Bellusci M, Martinelli A, D'Ilario L, Piozzi A. Antibiotic delivery polyurethanes containing albumin and polyallylamine nanoparticles. European journal of pharmaceutical sciences : official journal of the European Federation for Pharmaceutical Sciences. 2009 Mar 2;36(4-5):555-64. PubMed PMID: 19136061.
43. Luppi B, Bigucci F, Cerchiara T, Mandrioli R, Di Pietra AM, Zecchi V. New environmental sensitive system for colon-specific delivery of peptidic drugs. International journal of pharmaceutics. 2008 Jun 24;358(1-2):44-9. PubMed PMID: 18359586.
44. Mok H, Kim HJ, Park TG. Dissolution of biomacromolecules in organic solvents by nano-complexing with poly(ethylene glycol). International journal of pharmaceutics. 2008 May 22;356(1-2):306-13. PubMed PMID: 18313870.

45. Desai MP, Labhasetwar V, Amidon GL, Levy RJ. Gastrointestinal uptake of biodegradable microparticles: effect of particle size. Pharmaceutical research. 1996 Dec;13(12):1838-45. PubMed PMID: 8987081.
46. Immordino ML, Dosio F, Cattel L. Stealth liposomes: review of the basic science, rationale, and clinical applications, existing and potential. Int J Nanomedicine. 2006;1(3):297-315. PubMed PMID: 17717971. Pubmed Central PMCID: PMC2426795.
47. Czeslik C, Winter R, Rapp G, Bartels K. Temperature- and pressure-dependent phase behavior of monoacylglycerides monoolein and monoelaidin. Biophysical journal. 1995 Apr;68(4):1423-9. PubMed PMID: 7787028. Pubmed Central PMCID: PMC1282037.

7.1.1. Books, papers, and other articles

48. Jone Anna. Liposomes: a short review. Journal of Pharmaceutical Sciences and Research. 2013; Vol 5(9):181-183 (http://jpsr.pharmainfo.in/Documents/Volumes/vol5issue09/jpsr05091304.pdf)
49. Jacob N. Israelachvili. Intermolecular and Surface Forces, Second edition. Harcourt Brace & Company, New York, 1998
50. J. P. Neves Silva, A. C. N. Oliveira, A. C. Gomes and M. E. C. D. Real Oliveira (2012). Development of Dioctadecyldimethylammonium Bromide/Monoolein Liposomes for Gene Delivery, Cell Interaction, Dr. Sivakumar Gowder (Ed.), ISBN: 978-953-51-0792-7, InTech, DOI: 10.5772/48603. Available from: http://www.intechopen.com/books/cell-interaction/development-of-dioctadecyldimethylammonium-bromide-monoolein-liposomes-for-gene-delivery
60. C.D.R.Oliveira et al. Application on monoolein as a new helper lipid in transfection. United states patent application publication. July 2011
61. Michnik, Anna; Michalik, K.; Kluczewska, A.; Drzazga, Zofia. Comparative DSC study of human and bovine serum albumin. Journal of Thermal Analysis & Calorimetry; 2006 April, Vol. 84 Issue 1, p113
62. H. C. Berg, "Random Walks in Biology". Extended Paperback Ed. ed. 1993, Princeton, NJ: Princeton University Press.
63. Malvern Instruments Ltd, Zetasizer Nanoseries User Manual; April 2013, MAN0485 issue 1.1
64. Anfinsen C. B. Principles that govern the folding of protein chain. Science 1973, 181, 223–230
65. Magalhaes, L.M., Nunes, C., Lucio, M., Segundo, M.A., Reis, S. and Lima, J.L. 2010, Nat Protoc, 5, 1823
66. Sreerama, N. & Woody, R.W. Computation and analysis of protein circular dichroism spectra. Methods Enzymol. 383, 318–351 (2004).
67. Greenfield, N. Using circular dichroism spectra to estimate protein secondary structure. Nat Protoc. 2006; 1(6): 2876–2890.
68. Grant E. Frahm, Terry D. Cyr, Daryl G. S. Smith, Lisa D. Walrond, and Michael J. W. Johnston, Investigation of the Differences in Thermal Stability of Two Recombinant Human Serum Albumins with 1,2-Dipalmitoyl-snglycero-3-phosphocholine Liposomes by UV Circular Dichroism Spectropolarimetry J. Phys. Chem. B 2012, 116, 4661−4670
69. Poly(D,L-lactide-co-glycolide) protein-loaded nanoparticles prepared by the double emulsion method--processing and formulation issues for enhanced entrapment efficiency.
70. F.H. Almeida; Encapsulation of Bovine Serum Albumin (BSA) in DODAB:MO (1:2) Liposomes for Enhanced Antigen Immunization. Master Thesis, Uminho
78. Royer, C. A. Chem. Rev. 2006, 106, 1769−1784.
79. J. P. Neves Silva, A. C. N. Oliveira, Marlene Lúcio, Andreia C. Gomes, P. J. G. Coutinho, and M. E. C. D. Real Oliveira. Colloids and Surface B. 2014. Accepted for publication. Tunable pDNA/DODAB:MO lipoplexes: the effect of incubation temperature on the lipoplexes structure and transfection efficiency

7.2. CONSULTED WEBSITES

71. News-medical.net. (2011). What is a liposome? http://www.news-medical.net/health/What-is-a-Liposome.aspx (assessed 05/03/2014)
72. News-medical.net. (2011) Liposome research. http://www.news-medical.net/health/Liposome-Research.aspx (assessed 05/03/2014)
73. Georges-Louis Friedli. INTERACTION OF SWP WITH BOVINE SERUM ALBUMIN (BSA) http://www.friedli.com/research/PhD/chapter5a.html? (assessed 02/05/2014)
74. Sigma-Aldrich. Albumin from bovine serum. Product information. 2000 February http://www.sigmaaldrich.com/content/dam/sigma-aldrich/docs/Sigma/Product_Information_Sheet/a7906pis.pdf (assessed 05/03/2014)
75. David W. Brooks, Intrinsic Fluorescence of Proteins and Peptides, http://dwb.unl.edu/Teacher/NSF/C08/C08Links/pps99.cryst.bbk.ac.uk/projects/gmocz/fluor.htm (accessed 03/03/2014)
76. Avanti Polar Lipids, Inc. Preparation of Liposomes. https://www.avantilipids.com/index.php?option=com_content&view=article&id=1384&Itemid=372 (assessed 10/04/2014)
77. Avanti Polar Lipids, Inc. Preparation of Multilamellar Liposomes. (LMV)https://www.avantilipids.com/index.php?option=com_content&view=article&id=1599&Itemid=380 (assessed 1/04/2014)